iScience

Article

Chronic low-dose rate irradiation induces transient hormesis effect on cyanobacterium *Limnospira indica*

Graphical abstract

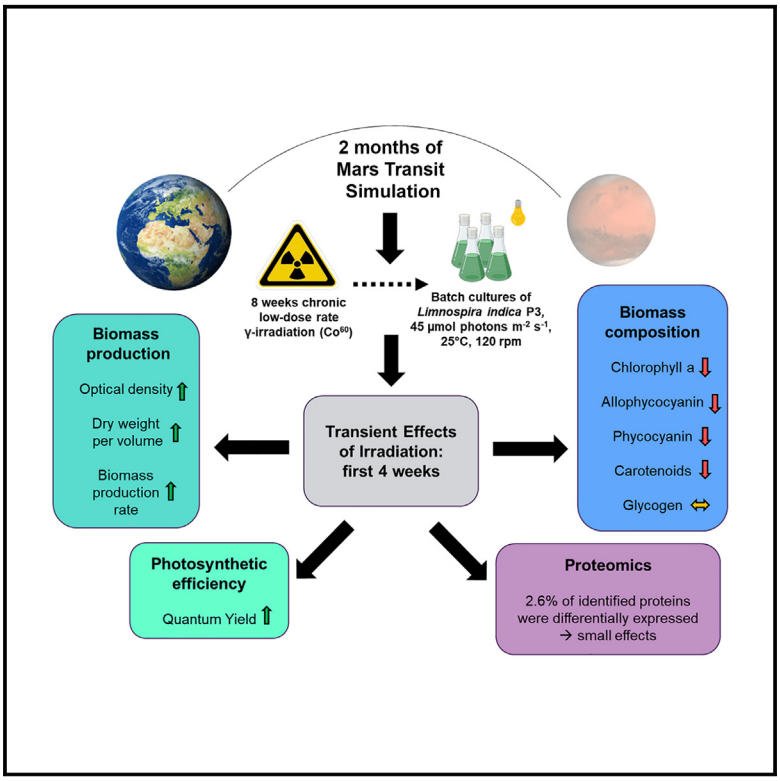

Highlights

- Eight weeks of low-dose rate γ-irradiation caused transient hormesis effect in *L. indica*
- The dry weight and cell density were higher in the irradiated cultures
- The pigment content was lower in the irradiated cultures
- The hormesis effect weared off after the first 4 weeks of radiation exposure

Authors

Jana Fahrion, Surya Gupta, Felice Mastroleo, Claude Gilles Dussap, Natalie Leys

Correspondence

natalie.leys@sckcen.be

In brief

Microbiology; Space sciences

Fahrion et al., 2025, iScience *28*, 111891
March 21, 2025
https://doi.org/10.1016/j.isci.2025.111891

CellPress

iScience

CellPress
OPEN ACCESS

Article

Chronic low-dose rate irradiation induces transient hormesis effect on cyanobacterium *Limnospira indica*

Jana Fahrion,[1,2] Surya Gupta,[1] Felice Mastroleo,[1] Claude Gilles Dussap,[2] and Natalie Leys[1,3,*]
[1]Microbial Biotechnology Unit, Nuclear Medical Applications, Belgian Nuclear Research Center SCK CEN, 2400 Mol, Belgium
[2]Université Clermont Auvergne, CNRS, Clermont Auvergne INP, Institut Pascal, 63100 Clermont-Ferrand, France
[3]Lead contact
*Correspondence: natalie.leys@sckcen.be
https://doi.org/10.1016/j.isci.2025.111891

SUMMARY

Cultures of *Limnospira indica* were exposed to low-dose rate γ-irradiation for 8 weeks to simulate 2 months of a Mars transit irradiation. Two experiments were conducted: in the first, 5% v/v inoculations were used over 2-week batches; in the second, 25% v/v inoculations over 1-week batches. The cultures were continuously illuminated (45 μmol photons m^{-2} s^{-1}, LEDs). A transient hormesis effect was observed in experiment 1, with irradiated cultures showing higher dry weight (1.88 ± 0.05 g L^{-1}) than controls (1.70 ± 0.06 g L^{-1}) on day 14. Irradiated cultures also had fewer pigments. Experiment 2 showed similar, though less pronounced, results. These findings suggest that *Limnospira indica* would not be negatively affected by cosmic radiation during Mars transit, though further validation under space flight conditions is needed. The resilience of *Limnospira indica* to chronic low-dose radiation supports its potential for oxygen and food production in life support systems for manned space missions.

INTRODUCTION

A reliable air, water, and food production is crucial for manned space flight to become more independent from Earth cargo supply. Regenerative life support systems aim to overcome these challenges using bioreactors for waste treatment, air and water revitalization, and food production. The MELiSSA project was initiated by the European Space Agency (ESA) in 1988 and uses, besides higher plants, the edible cyanobacterium *Limnospira indica* (previously known as *Spirulina* sp. and *Arthrospira* sp.) for air revitalization and as a supplementary food source.[1] The use of organisms like *L. indica* in space life support systems will require specific culture conditions that are not commonly used on Earth. These space conditions are tested in the precursor space flight experiments, ARTHROSPIRA-B and -C (ArtB and ArtC) of which the latter flew to the International Space Station (ISS) end 2024. In the ArtB and ArtC precursor flight experiments, *L. indica* is grown in photobioreactors designed for microgravity conditions and controlled by light-limiting conditions, meaning that the light intensity is the parameter by which the production of oxygen and biomass is controlled.[2] The start-up of the bioreactor in space includes a revival of the dormant inoculum (in dark and cold) and propagation in batch mode inside the space craft, because the inoculum cultures are stored dormant during upload to space (pre-launch, launch, and post-launch till reactivation). Thereafter the photobioreactors are run in semi-continuous mode (D = 0.01 h^{-1}) at 33°C and low light intensities (45–80 μmol photons m^{-2} s^{-1}) to induce slow growth allowing longer exposure to space conditions (e.g., cosmic irradiation, microgravity) while demanding low amounts of resources such as energy, medium, and crew time for feeding. It is known that light and temperature conditions have an impact on revival and biomass production kinetics and biomass composition.[3] The ArtB experiments showed that microgravity and low Earth orbit (LEO) irradiation onboard the ISS does not have a detrimental effect in fully mixed batch cultures. But the impact of long-term space conditions on *L. indica*, farther away from Earth, namely chronic low-dose irradiation, is not known yet. Characterizing the bioprocess that can be expected under these conditions is essential to detect possible changes in the cultures and to work toward a reliable oxygen and biomass production in a photobioreactor, on the ISS, and in the future, during manned Mars missions.

Space irradiation is one of the most serious challenges for manned missions as it increases the risk of cancer.[4,5] Cosmic irradiation composition and dose is not only highly dependent on the location in space (e.g., ISS or Mars), but also consists of several different types of ionizing radiation, each having possible different impacts on organisms.[6] In space, as well as on planetary bodies such as Mars, galactic cosmic rays (GCR) and solar energetic particles (SEP) are the two main sources of irradiation, both being mixtures of different types of ionising radiation. Cosmic radiation is composed of various particles, including protons, electrons, and atomic nuclei, as well as high-energy photons such as gamma rays able to penetrate deeply into matter. Protons make up the largest part of the

dose, followed by helium ions. Additionally, the irradiation dose highly depends on the solar cycle.[7] Recently, a detailed assessment of the irradiation environments on ISS, Moon, Mars, and in transit vehicles was published.[5] A dose rate of 20 μGy h^{-1} (or equivalent dose rate of 77 μSv h^{-1}) is the average dose rate on a transit mission to Mars, based on the measurements of the Curiosity rover mission.[8] This dose rate is higher when compared to the doserate of 16 μGy h^{-1} [9] (or 18–48 μSv h^{-1} [7]) on the moon surface or of 9 μGy h^{-1} (or ∼27 μSv h^{-1} [8]) on Mars surface and is therefore more likely to have a biological effect. For comparison, on the ISS, the measurements of personal badges worn by crewmembers usually show dose rates below 12.5 μGy h^{-1}, and on Earth, the general background irradiation dose rate is approximately 0.058 μGy h^{-1} [10] (or 0.420 μSv h^{-1}).[11] Even though ionizing radiation is physically correctly expressed as 'absorbed dose' in the SI unit Gray (Gy) (energy absorbed over mass, J kg^{-1}), when in contact with biology it is mostly expressed as 'equivalent dose' in the SI unit Sievert (Sv) (J kg^{-1}), considering the biological effectiveness of the radiation which is dependent on the radiation type and energy. Equivalent dose (in Sv) is a calculated value, as it cannot be practically measured, but the purpose of the calculation is to generate a value for comparison with observed health effects and to use it as a limiting quantity to specify exposure limits. The conversion from Gray to Sievert mainly depends on the type of irradiation and the irradiated tissue, therefore, the conversion factors are variable and need to be viewed in the correct context. For example, in humans, 1 Gray of space irradiation (GCR and SEP) on the surface of Mars corresponds to approximately 3 Sievert, while 1 Gray of gamma irradiation corresponds to approximately 1 Sievert.[8,12] Where applicable, both Gy and Sv values should be provided to give an idea of the ionizing irradiation dose as well as its effect on the tested biological system.[13,14]

In addition to space flight experiments, which are expensive and limited to a few per year worldwide, simulation experiments are conducted in laboratories on Earth. In these ground experiments, effects of ionizing irradiation and simulated microgravity on the organisms are tested to get a first idea on what to expect in orbit.[15–19] Due to limitations of test possibilities on ground, simulation experiments on Earth are always coming with drawbacks. The highly variable composition of space irradiation is very difficult to approximate in laboratory set-ups.[8] On Earth, irradiation experiments are usually performed with a single irradiation source, for example $Cobalt^{60}$, which decay emits low linear energy transfer (LET) gamma irradiation, with an energy of about 1.17 and 1.33 mega-electron volts (MeV).[20,21] Low LET radiation typically causes damage through interactions with water molecules in cells and indirect ionization by producing free radicals and reactive oxygen species.[22,23] Even though these single-source experiments only approximate space conditions, they are still useful to get a first understanding of possible outcomes in space and provide insight to metabolic adaptations of the biological systems and stress response pathways. So far, only experiments with much higher cumulative doses (500–5000 Gy) have been performed on cyanobacterium *Limnospira indica* (e.g.,[24–26]), emphasizing the need for research in low-dose ranges. Additionally, long term irradiation experiments on cyanobacterial cultures are still very rare,[27] as most works aim for high and acute doses to induce strong biological damage which are more likely to reveal stress response pathways in a cost and time saving manner. Space flight experiments such as the ArtB and ArtC experiments on the other hand are exposed to chronic low-dose irradiation on the ISS, and the same applies for future life support systems. The impact of chronic radiation exposure on active cell cultures over multiple generations at dose rates relevant for space, is not well known, as facilities to do such long-term tests are rare and expensive, and biological test set-ups in irradiation facilities (e.g., providing controlled humidity, temperature and light) are technically challenging. Chronic exposure to sublethal doses of radiation nevertheless have an impact on growth and biomass composition.[25,28] Exposure to low doses of ionizing radiation can have a hormesis effect.[29] Hormesis is defined by Mattson[30] as "a process in which exposure to a low dose of a chemical agent or environmental factor that is damaging at higher doses induces an adaptive beneficial effect on the cell or organism". It can not only originate from irradiation, but also from all typically damaging physical, chemical, and biological parameters, such as antibiotics, toxins or mechanical stress. For example, Liu et al.[31] showed a hormetic effect of amoxicillin (antibiotics) on the cyanobacterium *Microcystis aeruginosa*.

This paper provides an overview of the impact of chronic, low-dose gamma irradiation on *Limnospira indica* PCC8005 P3 in a consecutive batch set-up over a 2-month period (56 days), mimicking a fifth of a one-way trip to Mars (ca. 10 months or ∼300 days). Growth parameters, photosynthetic activity and pigment composition were monitored. This was completed by a whole proteome analysis of these samples in an attempt to unravel the metabolic pathways affected by the 8 weeks of Mars transit flight simulation. The results presented in this study are necessary in the ongoing development of life support systems for space applications and provide first indications on the appropriate expectations on the behavior of *Limnospira indica* in a life support system on the way to Mars.

RESULTS

Photosynthetic biomass production under continuous illumination and chronic irradiation

Figure 1 shows the cell density, measured by optical density at 770nm (OD_{770nm}) of the irradiated and control cultures of both experiments and shows the density range of the two different experiments. In experiment 1 (Figure 1A), the OD_{770nm} range between the start (lowest OD_{770nm}) and end of a batch (highest OD_{770nm}) was up to 1.8. The average overall OD_{770nm} value was 0.80 ± 0.62. Experiment 2 had a narrower range of approximately 1.0 between the lowest and highest OD_{770nm} value and yielded an average OD_{770nm} of 1.03 ± 0.33 (Figure 1B). Thus, the cell density during radiation exposure was lower in the beginning and higher at the end of a batch, in experiment 1 compared to experiment 2. The variation in pH levels, and thus carbon source availability as bicarbonate, is also much higher in experiment 1 (pH between 9.6 and 11.2), compared to experiment 2 (pH between 9.7 and 10.2) (supplementary data Figure S1). Figure 1A and Figure 2A show that the irradiated cultures grew

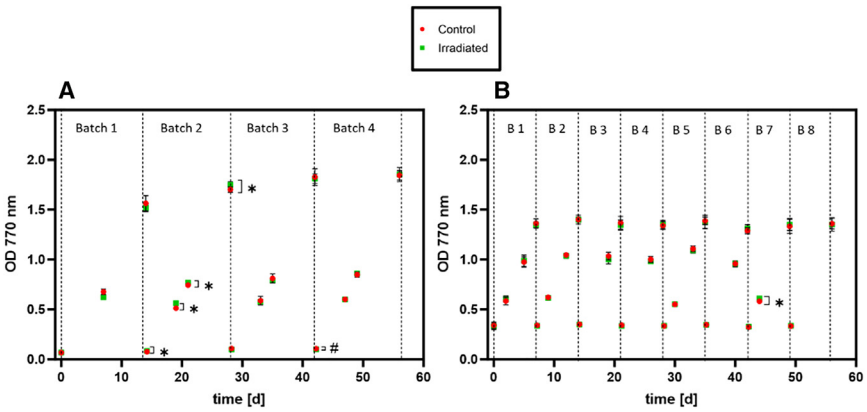

Figure 1. Absorbance measurements at 770 nm of the irradiated (green) and non-irradiated control (red) cultures of *L. indica*

(A) Experiment 1, (B) Experiment 2. Dotted line: End of Batch. Values are shown as mean ± SD, for 4 biological replicates measured with 3 technical replicates each ($n = 12$). Significance was tested at each time point using Mann-Whitney-U tests; the threshold for significance was $p < 0.05$. *: Irradiated cultures significantly higher than non-irradiated control, #: irradiated cultures significantly lower than non-irradiated control.

faster (confirmed in OD and dry weight measurements (DW)) in the first 4 weeks, i.e. in the first and second batch, of experiment 1. In experiment 2, a similar trend was only observed in DW after 4 weeks, i.e. in batch 4 (Figure 2B). Additionally, the biomass production rates (r_X) were calculated for each batch, based on the dry weight (Table 1). Only batch 4 of experiment 1 showed a significantly higher r_X in the irradiated cultures, all other time points were non-significant. Nevertheless, all r_X values were higher in the irradiated cultures in the first experiment. In summary, no negative impact of chronic 85.2 μSv h^{-1} (experiment 1) and 63.5 μSv h^{-1} (experiment 2) of γ-rays on the growth of *Limnospira indica* was found, and a transient hormesis effect was detected in the first 4 weeks of culturing.

Photosynthesis efficiency under chronic low-dose irradiation

Figure 3 shows the fraction of long and highly pigmented trichomes ('P1' cells) in the culture, expressed as percentage (% P1), measured by flow cytometry. The %P1 is similar for the non-irradiated control and irradiated cultures at most time points. Nevertheless, in 3 sampling time points, i.e., at the end of batch 1 and in the middle of batch 4 (experiment 1), and the end of the first batch of experiment 2, the irradiated cultures contained significantly more P1 cells than the non-irradiated cultures.

The quantum yield (QY) of photosynthesis determined for the (dark adapted) cultures of both experiments is shown in Figure 4. At 3 sampling time points, i.e., in batch 2 and 4 of experiment 1, and in batch 6 of experiment 2, the irradiated cultures had a higher QY than the control cultures.

Biomass composition under chronic low-dose irradiation

In both irradiation experiments, several analysis time points showed a significantly lower photosystem pigment content in the irradiated cultures, compared to the non-irradiated control cultures (Figure 5). The same trend can be seen in the total carotenoids content (Figure 6). Interestingly, in experiment 1 the chlorophyll *a*, allophycocyanin and phycocyanin contents of the irradiated cultures were found to be lower in the irradiated cultures in the first two and a half batches, i.e. first 5 weeks of cultivation. In experiment 2, the pigment contents of irradiated cultures are more similar to control cultures; although, a few time points indicated again a lower pigment content in the irradiated cultures, compared to the control cultures, similar to experiment 1.

In general, the glycogen content of all batch cultures was low (< 10% w/w, mg glycogen/mg DW) (Figure 7). The glycogen content per dry weight in the culture was highest in the middle of a batch, and values above 5% w/w were reached in the middle of batch 3 and 4 in experiment 1. At the end of a batch values of approximately 2.5% w/w were found. In both experiments,

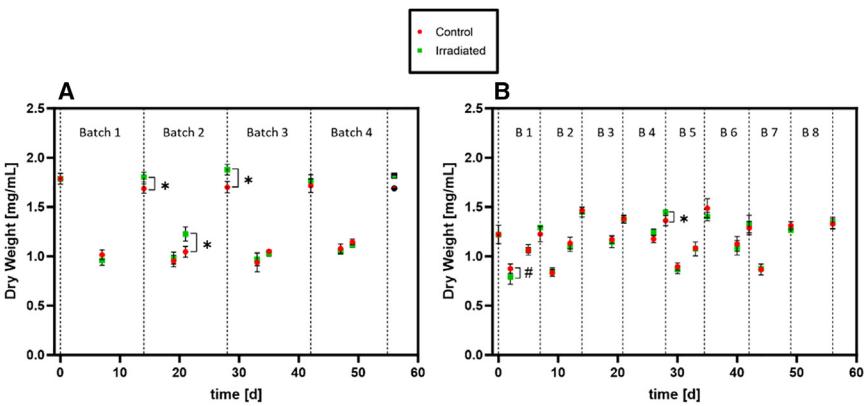

Figure 2. Dry weight measurements of the irradiated (green) and non-irradiated control (red) cultures of *L. indica*

(A) Experiment 1, (B) Experiment 2. Dotted line: End of Batch. Values are shown as mean ± SD, for 4 biological replicates measured with 3 technical replicates each ($n = 12$). Significance was tested at each time point using Mann-Whitney-U tests; the threshold for significance was $p < 0.05$. *: Irradiated cultures significantly higher than non-irradiated control, #: irradiated cultures significantly lower than non-irradiated control.

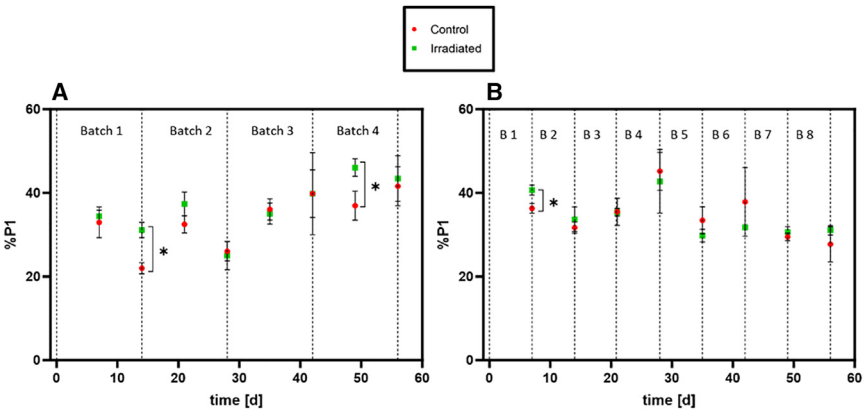

Figure 3. Fraction of long and highly pigmented trichomes ('P1' cells) in the culture (%P1), measured by flow cytometry, of the irradiated (green) and non-irradiated control (red) cultures of *L. indica*

(A) Experiment 1, (B) Experiment 2. Dotted line: End of Batch. Values are shown as mean ± SD ($n = 4$). Significance was tested at each time point using Mann-Whitney-U tests; the threshold for significance was $p < 0.05$. *: Irradiated cultures significantly higher than non-irradiated control.

the glycogen content of irradiated and non-irradiated control cultures was similar (Figure 7). Only the last time point of experiment 1 showed a significantly lower glycogen content in the irradiated cultures.

Proteomic analysis of irradiated cultures

In both irradiation experiments, a proteomic analysis was performed to elucidate the metabolic pathways and cellular processes of *L. indica* which are impacted by chronic low-dose γ-irradiation. Two time points were assessed: 4 weeks after start of the experiments (= middle of experiment) and 8 weeks after the start of the experiments (= end of experiment). In the first experiment, 1,268 proteins were identified when both time points (4 and 8 weeks) were combined and quantified, which corresponds to 20% of the total theoretical proteome, when considering the 6,345 protein coding sequences identified in the *L. indica* PCC8005 genome via the MaGe platform.[32] In the second experiment, 1,170 proteins were identified when both time points were combined and quantified, which is 18% of the total theoretical proteome. The full datasets are available via ProteomeXchange with identifier PXD051709.

In Table 2, an overview of the differentially expressed proteins at the investigated timepoints can be found. The percentages of differentially expressed proteins per total identified proteins show that the proteomic changes induced by irradiation were little. For example, in experiment 1, after 4 weeks, 21 proteins were found upregulated and 12 downregulated in the irradiated cultures compared to the non-irradiated culture, meaning only 1.7% and 0.9% of the found proteins were differentially expressed. A large portion of the differential expressed proteins, are proteins of unknown function (not annotated).

Table 3 shows all annotated differentially expressed proteins after 4 weeks (batch 2 of experiment 1; batch 4 of experiment 2) and 8 weeks (batch 4 of experiment 1; batch 8 of experiment 2) of chronic low dose γ-irradiation.

DISCUSSION

In the presented experiments, the *L. indica* cultures were irradiated for a total of 8 weeks, resulting in cumulative doses of 94.6 mGy and 70.6 mGy. Dose rates of 70.4 μGy h^{-1} (or 85.2 μSv h^{-1}, Co^{60} γ-rays, experiment 1) and 52.5 μGy h^{-1} (or 63.5 μSv h^{-1}, Co^{60} γ-rays, experiment 2) were used to simulate the first 2 months (8 weeks) of a ca. 10-month (ca. 300 days) during transit flight to Mars. Ideally the full 10-month duration should have been tested, but this was practically and economically not feasible in the irradiation facility used. Chronic low-dose Co^{60} γ-irradiation of photosynthetic active cultures of *Limnospira indica* PCC8005 strain P3 caused a higher cell density (OD_{770nm}), dry weight per volume (DW), a higher fraction of long and highly pigmented 'P1' cells (which are essential for revival of the culture after freezing), a higher efficiency with which absorbed light is used for photochemistry in PSII (a higher photosynthetic quantum yield (QY)), and a lower pigment content per dry weight (lower content of chlorophyll *a*, allophycocyanin, phycocyanin and carotenoids) in several time points. In experiment 1, more significantly different radiation effects were detected. The OD and DW analysis, as well as the %P1 and QY analysis, showed significant differences from end of batch 1 to end of batch 2 (Figures 1A, 2A, 3A and 4A). A decrease in pigment content in

Table 1. Biomass production rates of *L. indica* in irradiation experiments 1 and 2, calculated based on the measured dry weights (via linear regression)

rX (exp. 1) [g L^{-1} d^{-1}]	Batch 1	Batch 2	Batch 3	Batch 4
Non-IR Control	0.096 ± 0.014	0.087 ± 0.012	0.089 ± 0.014	0.070 ± 0.009
IR	0.121 ± 0.014	0.098 ± 0.012	0.093 ± 0.014	0.090 ± 0.010[a]

rX (exp. 2) [g L^{-1} d^{-1}]	Batch 1	Batch 2	Batch 3	Batch 4	Batch 5	Batch 6	Batch 7	Batch 8
Non-IR Control	0.069 ± 0.019	0.125 ± 0.020	0.104 ± 0.041	0.094 ± 0.046	0.114 ± 0.034	0.081 ± 0.072	0.089 ± 0.019	N/A
IR	0.099 ± 0.019	0.119 ± 0.024	0.115 ± 0.049	0.102 ± 0.029	0.104 ± 0.026	0.121 ± 0.082	0.078 ± 0.006	N/A

Values are shown as mean ±95%CI. Statistical significance was assessed based on overlapping 95%CI. N/A: data not available.
[a]irradiated (IR) cultures had a significantly higher biomass production rate compared to the non-irradiated (Non-IR Control) cultures.

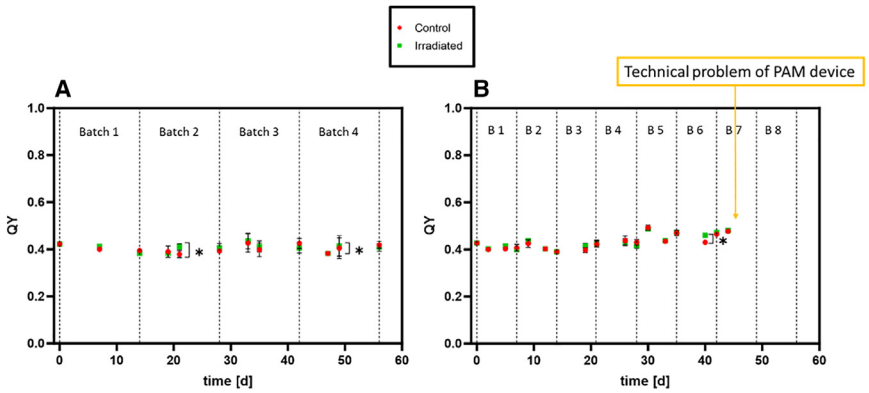

Figure 4. Photosynthesis quantum yield (QY) of the irradiated (green) and non-irradiated control (red) cultures of *L. indica*

(A) Experiment 1, (B) Experiment 2. Dotted line: End of Batch Values are shown as mean ± SD (n = 4). Significance was tested at each time point using Mann-Whitney-U tests; the threshold for significance was $p < 0.05$. *: Irradiated cultures significantly higher than non-irradiated control.

the irradiated cultures was detected from the start of the experiment until the mid of batch 3 (Figures 5A–5C and 6A). This effect was reversed in the case of allophycocyanin and phycocyanin from the end of batch 3 onwards, and these antenna pigment contents were higher in the irradiated cultures in batch 4. The chlorophyll and carotenoids contents were lower in the irradiated cultures from start to end of the first experiment. The glycogen content of the biomass was not affected by irradiation in both experiments (Figure 8).

Radiation susceptibility was influenced by the average cell density in the culture (OD_{770nm} = 0.80 ± 0.62 in experiment 1 and 1.03 ± 0.33 in experiment 2). In experiment 1, the cells were exposed to a higher variation of culture densities, because of the low (5%) inoculation at the start of a batch and the longer culturing time (2 weeks vs. 1 week). Thus, these cultures were exposed to a stronger variation in light to cell ratio, and had different cell densities during irradiation exposure, especially in the first days of cultivation. Additionally, the general dose rate was slightly higher in the first experiment (Experiment 1 at 70.4 μGy h^{-1} (or 85.2 μSv h^{-1}) and experiment 2 at 52.5 μGy h^{-1} (or 63.5 μSv h^{-1})). The irradiated cells in experiment 1 where impacted stronger than in experiment 2.

In general, the literature on the impact of low-dose rate irradiation on cyanobacteria is very limited. Nevertheless, there are previous studies on *Limnospira* strains using higher γ-irradiation dose rates, but in an acute instead of chronic set-up, and mostly in the dark. Tests with very high dose rates of 600 Gy h^{-1} and 527 Gy h^{-1} (acute irradiation, in the dark) were able to show that *Limnospira indica* PCC8005 is highly irradiation resistant and able to regrow after a total cumulative dose between 2100 Gy and 6400 Gy (γ-irradiation, Co^{60}), depending on the specific strain used.[24,25] Badri et al.[25] showed that the QY of

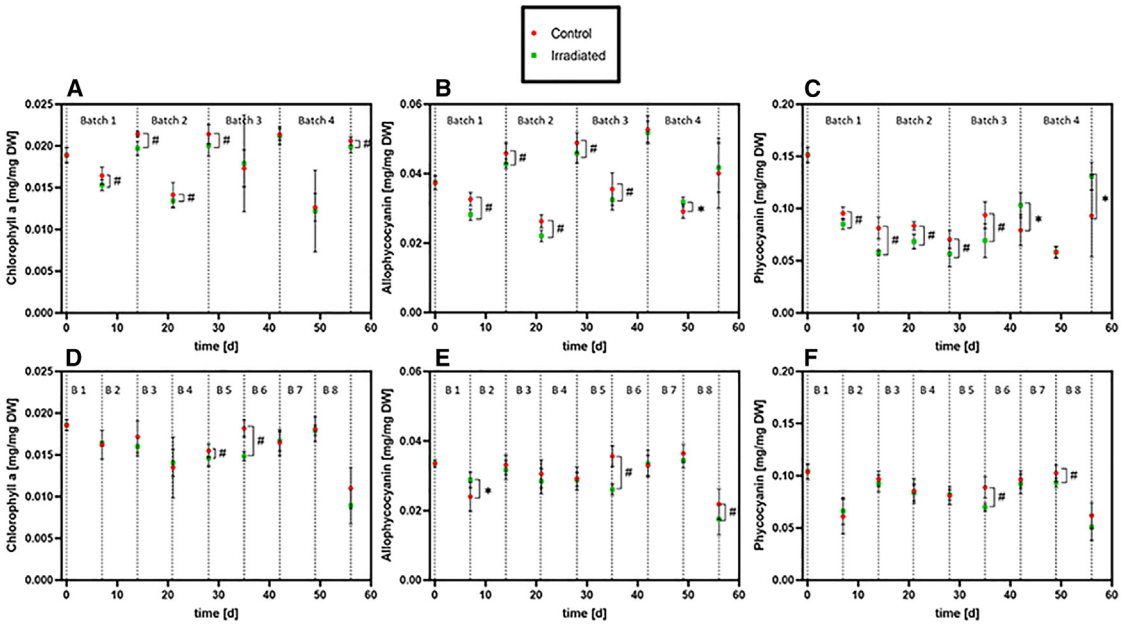

Figure 5. Pigment analysis of irradiated (green) and non-irradiated control (red) cultures of *L. indica*

Results of experiment 1 in the top row (A–C), and of experiment 2 in the bottom row (D–F). (A, D) chlorophyll *a*; (B and E) allophycocyanin; (C and F) phycocyanin. Values are shown as mean ± SD, for 4 biological replicates measured with 3 technical replicates each (n = 12). Mann-Whitney-U tests were performed for each time point to assess statistical significance; the threshold for significance was $p < 0.05$. *: Irradiated cultures significantly higher than non-irradiated control, #: irradiated cultures significantly lower than non-irradiated control.

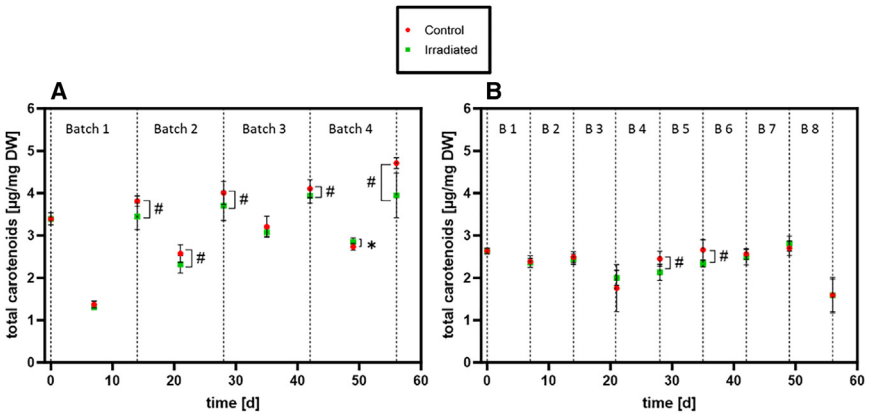

Figure 6. Total carotenoids content of the irradiated (green) and non-irradiated (red) cultures of L. indica

(A) Experiment 1, (B) Experiment 2. Dotted line: End of Batch. Values are shown as mean ± SD (n = 4). Significance was tested at each time point using Mann-Whitney-U tests; the threshold for significance was $p < 0.05$. #: irradiated cultures significantly lower than control.

Limnospira indica decreases significantly immediately after an acute cumulative dose of 1600 Gy gamma rays. Allophycocyanin and phycocyanin contents decreased from cumulative dose of 3200 Gy onwards, while the chlorophyll *a* content stayed stable up to a cummulative dose of 6400 Gy. In their RNA analysis, a strong decrease in the expression of the genes involved in the photosynthetic apparatus and carbon fixation was found after exposure to 3200 and 5000 Gy. Photosynthesis and electron transport are the main source of reactive oxygen species (ROS) under non-irradiated, photosynthetic growth conditions. Thus, a decrease in the expression of the related genes at high irradiation levels can be interpreted as a safety measure to avoid additional production of ROS. Additionally, an increased expression of thiol-based antioxidant systems, such as glutathione, was observed.[25] Protection from high ROS levels by accumulation of small antioxidants molecules such as glutathione, carotenoids, and low-molecular-weight Mn^{2+} complexes has been reported for several highly irradiation resistant organisms such as *Halobacterium salinarum* and *Deinococcus radiodurans*. However, the specific mechanisms of ROS protection for photosynthetic organisms such as cyanobacteria, plants and algae are not fully elucidated yet.[25,33,34]

The experiments with *L. indica* of the present study focused on the effects of irradiation during chronic low-dose rate irradiation, making direct comparisons to acute high dose rate irradiation studies difficult. No lethal effect was expected for the low dose rates used in the present study (i.e., 70.4 µGy h^{-1} and 52.5 µGy h^{-1}). Nevertheless, an impact of irradiation on the cultures was detected, even when non-lethal dose rates were used. In the present study, a transient irradiation hormesis was detected in experiment 1. Previous studies found similar growth stimulating effects of ionizing radiation on other cyanobacteria. Moussa et al.[26] found indications of hormesis effects on *Spirulina platensis* at an acute high cumulative dose of 2000 Gy of gamma rays (Co^{60} source). They found that not only the growth rates increased, but also chlorophyll A and carotenoid production was higher during the post-irradiation recovery phase (at 60 µmol photons m^{-2} s^{-1}). The higher carotenoid content could be attributed to the high antioxidant activity which is needed to keep the ROS levels under control after such high irradiation doses. Additionally, a higher ribulose-1,5-bisphosphate-carboxylase/oxygenase (RuBisCO) and phosphoenol pyruvate carboxylase activity was found in the irradiated cells, indicating a faster rate of carbon fixation after the irradiation. On the other hand, when *Arthrospira platensis* SAG 257.80 was irradiated in the dark with an acute cumulative dose of 2500 Gy γ-irradiation, the post-irradiation regrowth cultures (grown at 70 µmol photons m^{-2} s^{-1}) showed a decrease in growth rate and pigment production.[35] At lower cumulative irradiation doses (0.5, 1.0 and 1.5 kGy), the biomass productivity and the chlorophyll A and phycobilin content was not significantly different from the controls. Increased carotenoid production was found for all tested irradiation doses (0.5, 1.0, 1.5, 2.0 and 2.5 kGy, Co source). A

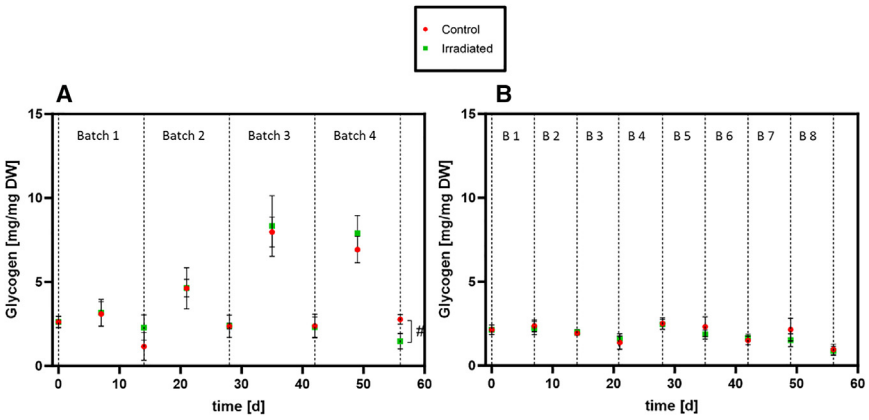

Figure 7. Glycogen content of the irradiated (green) and non-irradiated (red) cultures of L. indica

(A) Experiment 1, (B) Experiment 2. Dotted line: End of Batch. Values are shown as mean ± SD (n = 4). Significance was tested at each time point using Mann-Whitney-U tests (n = 4); the threshold for significance was $p < 0.05$. #: irradiated cultures significantly lower than control.

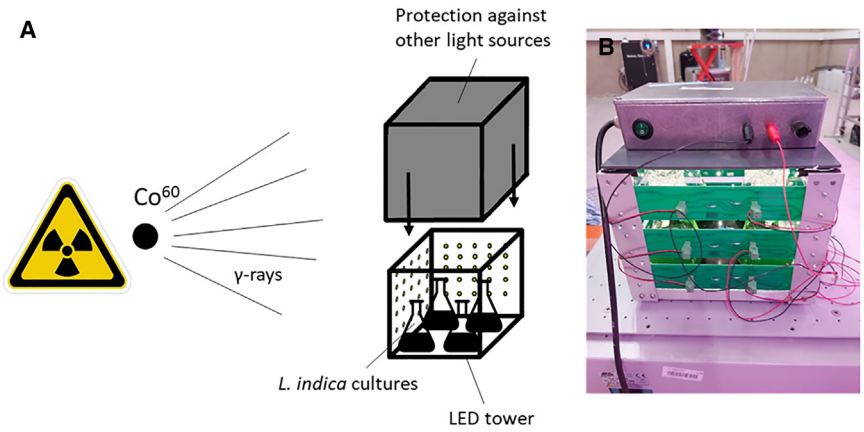

Figure 8. Set-up of the chronic low-dose rate irradiation experiments with *L. indica* batch cultures

(A) Schematic representation of experimental set-up, (B) Photo of the LED illumination tower (produced in-house, SCK CEN) on top of the orbital shaker (Edmund Bühler GmbH).

significant increase in total carbohydrate production was found at lower doses (0.5, 1.0 and 1.5 kGy). Phukan et al.[36] showed that acute exposure to low total doses of UV-C irradiation (6 and 12 mJ/cm^2) caused an increase in biomass production in recovering cultures of *Nostoc muscorum* Meg1, and also an increase in the pigment production in the days after the single low-dose UV-C exposure. In our experiments the *L. indica* cultures showed a decrease in antenna pigment content in the first 4 weeks (the hormesis period) during the chronic irradiation exposure, which was reversed toward the end of the experiments, where the IR cultures had higher pigment contents than the non-irradiated controls. This could indicate that a higher pigment production follows a low-pigment phase. To elucidate this effect, more chronic long-term irradiation experiments using photosynthetic organisms are needed, because acute set-ups usually investigate a recovery phase and not the impact of the ongoing irradiation environment. In the 1980s, low-light growth experiments (~1,051 Lux or ~14 μmol photons m^{-2} s^{-1} at surface level) on *Synechococcus lividus* in a shielded environment (Pb plates), to exclude background radiation, as well as a chronic low-dose rate irradiation with a thorium source (alpha decay) were performed.[27] They found that cultures which were shielded from natural background irradiation on Earth (by Pb plates) showed lower cell concentrations than (1) the control cultures exposed to the natural background irradiation (no extra source) and (2) the cultures that received an additional cumulative dose of 1.9 mGy given at a low-dose rate of 2.4 μGy h^{-1} for 33 days, which significantly increased the cell concentrations compared to the control cultures. They additionally found that the response of *Synechococcus lividus* to chronic low-dose irradiation depended on the light intensity as well as the growth phase of the culture inoculum. Additionally, to general scientific literature, also the FREDERICA database (https://www.frederica-online.org/mainpage.asp) was checked for possible comparative data. The database does not report on effects for phytoplankton at dose rates up to 1000 μGy h^{-1} and reports a minor stimulating effect on growth of *Synechococcus lividus* (1.2-fold), at dose rates between 0 and 50 μGy h^{-1} of alpha irradiation.

As mentioned above, the strong differences between the dose rate and total cumulative doses tested in the presented study and in literature makes it, however, challenging to compare the results or draw direct parallels. Also, it is important to keep in mind that the experiments with high dose rates usally use an acute set-up, in the dark, meaning the cultures are neither illuminated nor actively photosynthetically growing during the irradiation. Thus, the measurements of growth and biomass composition are done after the irradiation is finished, and therefore represent post-irradiation recovering cultures. Also, some of the reported effects in literature are contradictory, indicating that more experiments need to be performed to investigate the impact of acute and chronic irradiation. Nevertheless, while high dose rates of gamma irradiation can induce a stress response and finally cell death, low dose rates of gamma and alpha irradiation are sometimes found to be beneficial for growth and pigment production.

In the study presented here, a lower pigment per dry weight content was obtained during the first weeks of irradiation (Figure 3). It has been reported before that in light limiting culture conditions a decrease in antenna pigment concentration can be

Table 2. Overview of the number of differentially expressed proteins of *L. indica* in irradiation experiments 1 and 2, after 4 and 8 weeks of chronic irradiation exposure

Number of proteins	Experiment 1, after 4 weeks	Experiment 2, after 4 weeks	Experiment 1, after 8 weeks	Experiment 2, after 8 weeks
Total identified	1,251	1,246	1,148	1,153
Upregulated	21 (1.7%)	25 (2.1%)	12 (0.9%)	14 (1.2%)
Upregulated & Annotated	11 (0.9%)	17 (1.5%)	9 (0.7%)	9 (0.8%)
Downregulated	12 (0.9%)	20 (1.7%)	24 (1.9%)	16 (1.4%)
Downregulated & Annotated	5 (0.4%)	11 (0.9%)	17 (1.3%)	12 (1.0%)

The percentages are the number of differentially expressed proteins divided by the number of total identified proteins x100. Differential expressed proteins were identified based on a minimum of 2 peptides per protein, a log2 fold change (log2FC) of >0.585 or < −0.585, for up- and down regulated proteins respectively, and a p-value < 0.05.

Table 3. Differentially expressed proteins of *L. indica*, after 4 and 8 weeks of irradiation

Gene MageID	Product name	Protein Name	log2FC
Experiment 1, after 4 weeks			
ARTHROv5_10081|ID:18393500|	cell wall structural complex MreBCD (actin-like component)	MreB	0.67
ARTHROv5_11035|ID:18394454|	30S ribosomal subunit protein S19	RpsS	0.86
ARTHROv5_11043|ID:18394462|	50S ribosomal subunit protein L5	RplE	0.68
ARTHROv5_11060|ID:18394479|	peptide chain release factor RF-1	PrfA	1.57
ARTHROv5_11420|ID:18394839|	30S ribosomal subunit protein S16	RpsP	1.07
ARTHROv5_11557|ID:18394976|	phycobilisome 8.9 kDa linker polypeptide (phycocyanin-associated rod-capping linker protein)	CpcD	0.72
ARTHROv5_12037|ID:18395456|	gas vesicle structural protein	GvpC	0.69
ARTHROv5_30061|ID:18395890|	periplasmic solute binding protein precursor (modular protein)	–	1.58
ARTHROv5_30267|ID:18396096|	ATP-binding protein of ABC transporter	–	3.10
ARTHROv5_60299|ID:18398804|	dethiobiotin synthetase	BioD	1.11
ARTHROv5_60426|ID:18398931|	DNA topoisomerase I. (omega subunit)	TopA	1.60
ARTHROv5_10752|ID:18394171|	dihydrodipicolinate reductase	DapB	−0.77
ARTHROv5_40150|ID:18396844|	putative allergen V5/Tpx-1-like protein	–	−0.67
ARTHROv5_60416|ID:18398921|	isopentenyl-diphosphate delta-isomerase	Fni	−0.64
ARTHROv5_61125|ID:18399630|	heat shock protein A	HspA	−1.30
ARTHROv5_61129|ID:18399634|	peptidase S1 and S6, chymotrypsin/Hap	Hap	−0.72
Experiment 2, after 4 weeks			
ARTHROv5_10385|ID:18393804|	hydrogenase maturation protein (carbamoyl dehydratase)	HypE	0.80
ARTHROv5_10713|ID:18394132|	putative ABC-type sugar transport system (ATPase component)	–	1.61
ARTHROv5_10814|ID:18394233|	ATP phosphoribosyltransferase regulatory subunit	HisZ	0.60
ARTHROv5_11426|ID:18394845|	GDP-mannose 4,6-dehydratase	Gmd	0.85
ARTHROv5_11455|ID:18394874|	6-phosphofructokinase I	PfkA2	0.62
ARTHROv5_11938|ID:18395357|	aspartate kinase	Ask	0.81
ARTHROv5_30087|ID:18395916|	beta-lactamase-like protein (hydrolase)	–	1.28
ARTHROv5_30321|ID:18396150|	endopeptidase (cell wall lytic activity)	LytE	0.61
ARTHROv5_30345|ID:18396174|	GTP cyclohydrolase I	FolE2	1.73
ARTHROv5_30840|ID:18396669|	tetratricopeptide TPR_2 repeat protein	–	0.74
ARTHROv5_40254|ID:18396948|	succinate dehydrogenase (iron-sulfur subunit)	SdhB	0.92
ARTHROv5_40621|ID:18397315|	ABC Nitrate transport system (periplasmic component)	NrtA	0.63
ARTHROv5_40663|ID:18397357|	fragment of 3-dehydroquinate synthase (part 1)	AroB	0.74
ARTHROv5_41299|ID:18397993|	NAD-reducing hydrogenase (large subunit)	HoxH	0.76
ARTHROv5_60228|ID:18398733|	1-deoxy-D-xylulose-5-phosphate synthase	Dxs	1.11
ARTHROv5_60400|ID:18398906|	putrescine ABC transporter (ATP binding subunit)	PotG	1.06
ARTHROv5_61193|ID:18399698|	glycogen debranching enzyme	GlgX1	0.62
ARTHROv5_10143|ID:18393562|	thiazole biosynthesis protein	ThiG	−1.19
ARTHROv5_11995|ID:18395414|	polyphosphate kinase	Ppk	−2.58
ARTHROv5_20223|ID:18395782|	glyoxalase I, Ni-dependent	GloA	−0.86
ARTHROv5_30402|ID:18396231|	NAD+ dependent glycerol-3-phosphate dehydrogenase	GpsA	−0.85
ARTHROv5_41279|ID:18397973|	30S ribosomal subunit protein S21	RpsU	−0.59
ARTHROv5_41420|ID:18398114|	acetate kinase A	AckA	−0.81
ARTHROv5_50110|ID:18398246|	multimodular transpeptidase-transglycosylase	–	−1.60
ARTHROv5_50266|ID:18398402|	putative glycosyltransferase (group 1)	–	−0.99
ARTHROv5_60426|ID:18398931|	DNA topoisomerase I (omega subunit)	TopA	−0.68
ARTHROv5_60622|ID:18399127|	NifU domain-containing protein	–	−0.92
ARTHROv5_61133|ID:18399638|	short-chain dehydrogenase/reductase SDR	–	−1.10

(*Continued on next page*)

Table 3. *Continued*

Gene MageID	Product name	Protein Name	log2FC
Experiment 1, after 8 weeks			
ARTHROv5_10886|ID:18394305|	response regulator receiver domain protein (chemotaxis protein)	CheY4	1.05
ARTHROv5_11039|ID:18394458|	50S ribosomal protein L29	RpmC	0.73
ARTHROv5_11129|ID:18394548|	ferredoxin (2Fe-2S)	Fdx	0.93
ARTHROv5_11896|ID:18395315|	putative alcohol dehydrogenase	GroES	0.91
ARTHROv5_11964|ID:18395383|	glycosyl transferase group 1	–	1.35
ARTHROv5_11965|ID:18395384|	flavin reductase domain protein (FMN-binding)	–	0.74
ARTHROv5_12033|ID:18395452|	gas vesicle structural protein (short variant)	GvpC1	0.83
ARTHROv5_30209|ID:18396038|	histidyl tRNA synthetase	HisS	1.69
ARTHROv5_40235|ID:18396929|	photosystem I assembly related protein	Ycf37	1.10
ARTHROv5_10491|ID:18393910|	cytoplasmic alpha-amylase	AmyA	−0.64
ARTHROv5_10648|ID:18394067|	universal stress protein	UspA	−0.67
ARTHROv5_11049|ID:18394468|	preprotein translocase (membrane subunit)	SecY	−0.70
ARTHROv5_11707|ID:18395126|	adenine phosphoribosyltransferase	Apt	−0.72
ARTHROv5_11853|ID:18395272|	rfaE bifunctional protein	RfaE	−0.67
ARTHROv5_20109|ID:18395668|	S4 RNA-binding domain-containing protein	–	−0.66
ARTHROv5_20201|ID:18395760|	polyamine transporter subunit (periplasmic-binding component of ABC superfamily)	PotD1	−0.91
ARTHROv5_30263|ID:18396092|	glycosyl transferase (group 1)	–	−1.19
ARTHROv5_30648|ID:18396477|	putative methyltransferase (type 11)	–	−1.51
ARTHROv5_30849|ID:18396678|	protein transporter (type II protein secretion system complex)	–	−1.38
ARTHROv5_40204|ID:18396898|	putative phosphodiesterase/alkaline phosphatase D	–	−0.61
ARTHROv5_40755|ID:18397449|	putative ribonuclease Z	–	−1.58
ARTHROv5_60179|ID:18398684|	putative SAM-dependent methyltransferase	–	−0.75
ARTHROv5_60607|ID:18399112|	2-methyl-6-phytyl-1,4-hydroquinone methyltransferase	–	−0.84
ARTHROv5_60973|ID:18399478|	protein serine/threonine phosphatase	–	−0.68
ARTHROv5_61026|ID:18399531|	thiamine biosynthesis protein	ThiC	−2.21
ARTHROv5_61097|ID:18399602|	short chain dehydrogenase	–	−2.36
Experiment 2, after 8 weeks			
ARTHROv5_10266|ID:18393685|	central regulator of carbon metabolism (putative)	–	1.64
ARTHROv5_10626|ID:18394045|	putative thiosulfate:cyanide sulfurtransferase (rhodanese)	GlpE	1.15
ARTHROv5_11290|ID:18394709|	spermidine synthase (putrescine aminopropyltransferase)	SpeE	1.36
ARTHROv5_11768|ID:18395187|	FeS assembly protein	SufD	1.42
ARTHROv5_20104|ID:18395663|	peptide chain release factor 2	PrfB	1.38
ARTHROv5_20189|ID:18395748|	S-methyl-5′-thioadenosine phosphorylase	MtaP	0.74
ARTHROv5_41424|ID:18398118|	putative DnaJ-class molecular chaperone	DnaJ	0.99
ARTHROv5_60228|ID:18398733|	1-deoxy-D-xylulose-5-phosphate synthase	Dxs	0.80
ARTHROv5_61125|ID:18399630|	heat shock protein A	HspA	0.94
ARTHROv5_10226|ID:18393645|	glycolate oxidase (iron-sulfur subunit)	GlcF	−0.65
ARTHROv5_11357|ID:18394776|	cob(I)yrinic acid a,c-diamide adenosyltransferase	CobO	−0.90
ARTHROv5_11419|ID:18394838|	signal recognition particle protein component	Ffh	−0.74
ARTHROv5_11572|ID:18394991|	ATP-dependent Clp protease (ATP-binding subunit clpA homolog)	ClpC1	−0.95
ARTHROv5_11813|ID:18395232|	Chaperone protein	DnaJ	−0.59
ARTHROv5_11995|ID:18395414|	polyphosphate kinase	Ppk	−1.96
ARTHROv5_30444|ID:18396273|	PP2C/PPM-type Ser/Thr protein phosphatase	–	−0.67
ARTHROv5_40939|ID:18397633|	putative two component sulfate transporter	–	−1.60
ARTHROv5_41149|ID:18397843|	tryptophanyl-tRNA synthetase	TrpS	−3.21
ARTHROv5_50101|ID:18398237|	putative structural maintenance of chromosomes (SMC) protein	–	−1.00

(*Continued on next page*)

Table 3. *Continued*

Gene MageID	Product name	Protein Name	log2FC
ARTHROv5_50156|ID:18398292|	putative hemolysin-type calcium-binding toxin (RTX-like)	–	−0.81
ARTHROv5_61097|ID:18399602|	short chain dehydrogenase	–	−2.55

Positive Log2FC values: upregulated in the irradiated conditions, Negative Log2FC values: downregulated in the irradiated cultures. Only proteins that were identified with at least 2 peptides, a log2FC value of >0.585 or < −0.585, and a *p*-value below 0.05 were considered. Proteins of unknown function are not listed here (full data are available via ProteomeXchange with identifier PXD051709). Proteins were sorted following the MaGe ID.

correlated with a higher photosynthetic efficiency (higher quantum yield QY) in cyanobacteria, as it is a mechanism to optimize the balance between light absorption and energy utilization.[37] The lower number of pigments possibly arises from increased ROS levels due to γ-rays, triggering a similar response as a response to a higher light condition, i.e., less light limiting condition in the cultures. Cyanobacteria change their pigment composition based on the light conditions and a reduction of antenna pigments under higher light intensities was also previously shown for *L. indica* PCC8005 P3.[3] The reduction of pigment concentration led to a more optimized light harvesting versus energy processing in PSII, leading in general to a more effective photosynthesis under low dose rate irradiation. The increase in QY measured in the irradiated cultures supports this hypothesis (Figure 4). Mild increases in photosynthesis rates have already been shown for low-dose irradiation experiments with the water lentil plant *Lemna minor*.[38] The observed increase in biomass production, in combination with the decrease in pigments, can be explained by an overcompensation after a short period of disrupted electron homeostasis (reviewed for plants in Volkova et al.[39]). The disrupted electron homeostasis mainly arises from the interaction of the gamma rays with the water molecules, resulting in higher ROS and electron abundance.

The biomass composition was only slightly affected by the irradiation. While the glycogen content remained similar, the amount of pigments per dry weight was lower at several time points. These effects were more pronounced in the first experiment. In experiment 1, while the growth (OD, DW, r_X) and photosynthetic efficiency (%P1, QY) show an upwards trend, the pigment content decreased, likely as part of a natural response to higher ROS. However, all these effects were found to be small and transient, as most of the significant difference were only found in the first month (first 4 weeks) of irradiation exposure, indicating that an acclimation response occured afterwards.

While identifying and quantifying 1,268 and 1,170 proteins (18–20% of the protein coding sequences in the genome), the whole proteome analysis reported very few differentially expressed proteins between the irradiated and non-irradiated control cultures. This indicated a limited impact of the chronic low-dose γ-irradiation on the batch cultures. Nevertheless, a few interesting proteins were found to be differentially expressed.

Three proteins belonging to the polyamine transport and metabolism (PotG, PotD1, SpeE) were differentially expressed. The putrescine (1,4-diaminobutane) ABC transporter ATP binding subunit PotG was upregulated after 4 weeks in experiment 2, the polyamine transporter subunit PotD1 was downregulated after 8 weeks in experiment 1 and the spermidine (N-(3-aminopropyl)-1,4-diaminobutane) synthase SpeE was upregulated after 8 weeks in experiment 2. In cyanobacteria, polyamines such as putrescine and spermidine are involved in stress response mechanisms but their role in these stress response reactions is not fully elucidated yet.[40,41] In *Escherichia coli*, polyamines were proven to protect the cells from radiation induced DNA strand breaks.[42] This could indicate a connection between a shift in polyamine synthesis and transport and low-dose irradiation in *L. indica*. In experiment 1, after 8 weeks, the iron-sulfur (FeS) cluster containing protein ferredoxin (Fdx) was upregulated, an important electron transfer protein which is also part of cyclic electron transport,[43] and in experiment 2 after 8 weeks, the FeS assembly protein SufD was upregulated.[44] HypE and HoxH were both found to be upregulated in the irradiated cultures after 4 weeks in experiment 2. These proteins are part of the hydrogenase assembly responsible of producing H_2 from H^+, a pathway which is used as an electron sink.[45] Thus, different proteins related to ROS and electron handling where differentially expressed, supporting the assumption, that ionising radation impacts the redox status and balance of the cells, and as such the metabolism and the growth and biomass composition of *L. indica*.

After the first month of exposure to radiation (week 4), a few ribosomal subunit proteins were found to be significantly upregulated (experiment 1), as well as a protein of the prokaryotic cytoskeleton, MreB (exp. 1), supporting the higher dry weight and cell density measurements. Also, CpcD, a linker polypeptide associated to the antenna construction (Experiment 1) and chromophore lyase CpcS were upregulated in the irradiated cultures (both experiments after 4 weeks). CpcS enzyme is responsible for attaching phycocyanobilin to phycobiliproteins,[46] and thus also involved in the antenna assembly, similar to the CpcD linker polypeptide. The upregulation of both enzymes indicates a shift toward a higher antenna assembly, which support our observation that the lower antenna pigment content in the irradiated cultures was reversed toward the end of the experiments (Figure 5). Overall, this suggests a higher rate in protein biosynthesis in combination with a change in antenna assembly in the irradiated cultures.[47] Some proteins related to sugar metabolism were found to be upregulated in the irradiated cultures, such as 1-deoxy-D-xylulose-5-phosphate synthase (Dxs), GDP-mannose 4,6-dehydratase (Gmd), 6-phosphofructokinase (PfkA2) and succinate dehydrogenase iron-sulfur subunit (SdhB) (in exp. 2, after 4 weeks), indicating a small shift in metabolic routes. Nevertheless, no related proteins of an operon or full pathway were found to be differentially expressed, therefore the evidence for a change in sugar utilization is poor. Additionally, the polyphosphate kinase Ppk was found to be downregulated in irradiated cultures. This enzyme is involved in the synthesis of polyphosphate as intracellular P-stock which is usually used as a form of energy storage.[48] It indicates cells halted polyphosphate synthesis to leave Pi to support the higher biomass synthesis. Also, proteins involved in the thiamine (vitamin B1)

biosynthesis were found to be downregulated in irradiated cultures. This includes the thiazole biosynthesis protein ThiG and the thiamine biosynthesis protein ThiC.[49] Thiamine diphosphate is derived from thiamine, and is needed as cofactor in several metabolic reactions, such as the TCA cycle[50,51] and plays an essential role in carbohydrate metabolism as a cofactor of the pyruvate dehydrogenase.[52] In future irradiation experiments, metabolomic analyses of thiamine (vitamin B1) could be added to confirm this result. Similarly, analysis of folate (vitamin B9) could be considered, because of the strong upregulation of FolE2 (GTP cyclohydrolase I) which was detected after 4 weeks in experiment 2. The role of folate is mainly to carry one-carbon units and it is involved in the synthesis of L-methionine, L-serine and glycine and part of the DNA synthesis.[53–55] Dethiobiotin synthetase BioD was found to be upregulated after 4 weeks in experiment 1. This enzyme is part of the biotin (Vitamin B7) metabolism. Biotin is needed for the enzymes pyruvate carboxylase and acetyl-CoA carboxylase (which is needed for fatty acid production in membrane synthesis) and the TCA cycle.[55,56] In a future life support system including *L. indica*, the possible changes in vitamin contents under irradiation need to be monitored and understood to exclude a negative effect on the nutritive value.

After the second month of radiation exposure (8 weeks), only 1 ribosomal subunit was upregulated, indicating that the increase in biomass production rate was a reversible effect, and evolved back to base line (similar as in non-irradiated cultures), as it was also be seen in the cell density (OD) and dry weight measurements which were no longer different from controls (Figures 1 and 2). Nevertheless, a putative central regulator of carbon metabolism was upregulated (after 8 weeks, in experiment 2), indicating possible changes in the carbon utilization routes. The 1-deoxy-D-xylulose-5-phosphate synthase (Dxs) was still differentially expressed (upregulated) in week 8 as in week 4, suggesting a continued small increase in isoprenoid biosynthesis, which are, for example, needed as quinones in the electron transport chain.[57,58] And again, the polyphosphate kinase protein Ppk was found to be still downregulated, similar as after 4 weeks (experiment 2), suggesting a remaining shift in energy storage pathways.[48] Also, the thiamine (vitamin B1) biosynthesis was still also found to be downregulated in the irradiated cultures. The chemotaxis protein CheY4 was found upregulated in irradiated cultures (after 8 weeks, in experiment 1). The CheY proteins are suspected to be involved in phototaxis of *Synechocystis*.[59] Similarly, the gas vesicle protein GvpC was found to be upregulated in experiment 1 after 4 and 8 weeks. This protein is part of the gas vesicles inside the *L. indica* cells which are responsible for the adaptable buoyancy of the organism, and thus also part of phototaxis.[60]

In summary, only a very small fraction of proteins was found to be differentially expressed indicating a minor impact of the low-dose γ-irradiation on the proteome of *L. indica*. Nevertheless, some interesting differences could be detected, suggesting a higher ROS status inside the irradiated cultures. In conclusion, chronic exposure to low-dose rate of Co^{60} γ-irradiation over 2 months does not negatively impact batch cultures of the cyanobacterium *Limnospira indica* PCC8005 P3, when grown under continuous illumination at low light intensity. When a lower cell density was used (experiment 1), a transient hormesis effect was detected in the first four weeks of irradiation. During this period, biomass production rate (based on optical density and dry weight) and maximum photosynthetic quantum yield were higher in the irradiated cultures compared to the non-irradiated cultures. The pigment contents (% w/w) were lower. After 2 months, toward the end of the experiment (weeks 6–8), the irradiated and control cultures showed hardly any differences anymore, indicating a transient response followed by adaptation of *Limnospira indica* PCC8005 P3 batch cultures to chronic low-dose γ-irradiation. These results provide a first indication that active photosynthetic cultures of *Limnospira indica* PCC8005 P3 are robust to chronic ionizing radiation, supporting their potential for applications in life support systems for a transit flight to Mars. However, more ground experiments using high-energy particle sources that more closely mimic cosmic rays, and eventually deep space flight experiments, are the logical next step to validate the robustness of *Limnospira indica* PCC8005 P3 to space radiation.

Limitations of the study

The irradiation source ($Cobalt^{60}$) used in this study is only emitting gamma irradiation, but the irradiation environment in space is much more complex and consists of, e.g., protons, electrons, and atomic nuclei which could have additional or different effects on *Limnospira indica*. Additionally, the chronic exposure in these experiments was performed for 8 weeks (2 months), but a Mars transit flight takes approximately 10 months. Thus, accumulating effects of longer exposure times were not investigated in this study.

RESOURCE AVAILABILITY

Lead contact

Requests for resources and information should be directed to Dr. Natalie Leys (natalie.leys@sckcen.be).

Materials availability

The specific substrain *Limnospira indica* PCC8005 P3, which is used in these experiments, is originating from the private collection of the Belgian Nuclear Research Center (SCK CEN) and can be requested from the lead contact.

Data and code availability

The mass spectrometry proteomic data have been deposited to the ProteomeXchange Consortium via the PRIDE partner repository and are publicly available as of the date of publication. Accession numbers are listed in the key resources table. This paper does not report original code. Any additional information required to reanalyze the data reported in this paper is available from the lead contact upon request.

ACKNOWLEDGMENTS

The authors would like to thank Ms. Ilse Coninx and Ms. Laia Navarro Irun for their practical help in the laboratory. This work was funded via the SCK CEN PhD Grant of J.F., which is part of the ArtEMISS project, funded by BELSPO and ESA via the PRODEX program (grant agreement no. PEA 4000142717). The ArtEMISS project is part of the MELiSSA project of ESA (www.melissafoundation.org).

AUTHOR CONTRIBUTIONS

J.F., N.L., and C.D. designed the experimental set-ups; J.F. performed the experiments in the laboratory and wrote the first draft; N.L., C.D., F.M., and S.G.

contributed to reviewing and editing. F.M. and S.G. generated the proteomic data. All authors contributed to the article and approved the submitted version.

DECLARATION OF INTERESTS

The authors declare no competing interests.

STAR★METHODS

Detailed methods are provided in the online version of this paper and include the following:

- KEY RESOURCES TABLE
- EXPERIMENTAL MODEL AND STUDY PARTICIPANT DETAILS
- METHOD DETAILS
  - Optical density, dry weight and pH measurements
  - Flow cytometry
  - Photosynthesis quantum yield measurement
  - Pigment analysis
  - Glycogen analysis
  - Proteome analysis
- QUANTIFICATIONS AND STATISTICAL ANALYSIS

SUPPLEMENTAL INFORMATION

Supplemental information can be found online at https://doi.org/10.1016/j.isci.2025.111891.

Received: July 12, 2024
Revised: August 27, 2024
Accepted: January 22, 2025
Published: January 25, 2025

REFERENCES

1. Lasseur, C., Brunet, J., de Weever, H., Dixon, M., Dussap, C.G., Gódia, F., Leys, N., Mergeay, M., and Van Der Straeten, D. (2010). MELiSSA: The european project of closed life support system. Gravitational Space Biol. *23*.
2. Poughon, L., Laroche, C., Creuly, C., Dussap, C.G., Paille, C., Lasseur, C., Monsieurs, P., Heylen, W., Coninx, I., Mastroleo, F., and Leys, N. (2020). Limnospira indica PCC8005 growth in photobioreactor: model and simulation of the ISS and ground experiments. Life Sci. Space Res. *25*, 53–65. https://doi.org/10.1016/j.lssr.2020.03.002.
3. Fahrion, J., Dussap, C.G., and Leys, N. (2023). Biological oxygen production in Space: Assessment of the right conditions in cyanobacterial batch cultures. Front. Astronomy Space Sci. *10*, 121.
4. Durante, M., and Cucinotta, F.A. (2011). Physical basis of radiation protection in space travel. Rev. Mod. Phys. *83*, 1245–1281.
5. Berger, T., Matthiä, D., Burmeister, S., Zeitlin, C., Rios, R., Stoffle, N., Schwadron, N.A., Spence, H.E., Hassler, D.M., and Ehresmann, B. (2020). Long term variations of galactic cosmic radiation on board the International Space Station, on the Moon and on the surface of Mars. J. Space Weather Space Clim. *10*, 34.
6. Task Group on Radiation Protection in Space ICRP Committee 2; Dietze, G., Bartlett, D.T., Cool, D.A., Cucinotta, F.A., Jia, X., McAulay, I.R., Pelliccioni, M., Petrov, V., Reitz, G., and Sato, T. (2013). ICRP Publication 123: Assessment of radiation exposure of astronauts in space. Ann. ICRP *42*, 1–339.
7. Naito, M., Hasebe, N., Shikishima, M., Amano, Y., Haruyama, J., Matias-Lopes, J.A., Kim, K.J., and Kodaira, S. (2020). Radiation dose and its protection in the Moon from galactic cosmic rays and solar energetic particles: at the lunar surface and in a lava tube. J. Radiol. Prot. *40*, 947–961.
8. Hassler, D.M., Zeitlin, C., Wimmer-Schweingruber, R.F., Ehresmann, B., Rafkin, S., Eigenbrode, J.L., Brinza, D.E., Weigle, G., Böttcher, S., Böhm, E., et al. (2014). Mars' surface radiation environment measured with the Mars Science Laboratory's Curiosity rover. Science *343*, 1244797.
9. Spence, H.E., Golightly, M.J., Joyce, C.J., Looper, M.D., Schwadron, N.A., Smith, S.S., Townsend, L.W., Wilson, J., and Zeitlin, C. (2013). Relative contributions of galactic cosmic rays and lunar proton "albedo" to dose and dose rates near the Moon. Space Weather *11*, 643–650.
10. Charles, M. (2010). Effects of Ionizing Radiation: United Nations Scientific Committee on the Effects of Atomic Radiation: UNSCEAR 2006 Report, Volume 1—Report to the General Assembly, with Scientific Annexes A and B (Oxford University Press).
11. Odenwald, S., and Geyer, A. (2011). Mathematical Problems Featuring Radiation Effects Applications (National Aeronautics and Space Administration NASA).
12. Wakeford, R. (2004). The cancer epidemiology of radiation. Oncogene *23*, 6404–6428.
13. Ferrari, C., Manenti, G., and Malizia, A. (2023). Sievert or Gray: Dose Quantities and Protection Levels in Emergency Exposure. Sensors *23*, 1918.
14. Icrp (1990). Recommendations ofthe International Commission on Radiological Protection. Publication 60. Annex B. Ann. ICRP *21*, 1.
15. Verbeelen, T., Fernandez, C.A., Nguyen, T.H., Gupta, S., Aarts, R., Tabury, K., Leroy, B., Wattiez, R., Vlaeminck, S.E., Leys, N., et al. (2024). Whole transcriptome analysis highlights nutrient limitation of nitrogen cycle bacteria in simulated microgravity. NPJ Microgravity *10*, 3.
16. Senatore, G., Mastroleo, F., Leys, N., and Mauriello, G. (2020). Growth of Lactobacillus reuteri DSM17938 Under Two Simulated Microgravity Systems: Changes in Reuterin Production, Gastrointestinal Passage Resistance, and Stress Genes Expression Response. Astrobiology *20*, 1–14. https://doi.org/10.1089/ast.2019.2082.
17. Brungs, S., Egli, M., Wuest, S.L., M. Christianen, P.C., WA van Loon, J.J., Ngo Anh, T.J., and Hemmersbach, R. (2016). Facilities for simulation of microgravity in the ESA ground-based facility programme. Microgravity Sci. Technol. *28*, 191–203.
18. Mastroleo, F., Van Houdt, R., Atkinson, S., Mergeay, M., Hendrickx, L., Wattiez, R., and Leys, N. (2013). Modelled microgravity cultivation modulates N-acylhomoserine lactone production in Rhodospirillum rubrum S1H independently of cell density. Microbiology *159*, 2456–2466. https://doi.org/10.1099/mic.0.066415-0.
19. Mastroleo, F., Van Houdt, R., Leroy, B., Benotmane, M.A., Janssen, A., Mergeay, M., Vanhavere, F., Hendrickx, L., Wattiez, R., and Leys, N. (2009). Experimental design and environmental parameters affect Rhodospirillum rubrum S1H response to space flight. ISME J. *3*, 1402–1419. https://doi.org/10.1038/ismej.2009.74.
20. Reali, L., Gilbert, M.R., Boleininger, M., and Dudarev, S.L. (2023). Intense γ-photon and high-energy electron production by neutron irradiation: effects of nuclear excitations on reactor materials. PRX Energy *2*, 023008.
21. Pouget, J.P., Frelon, S., Ravanat, J.-L., Testard, I., Odin, F., and Cadet, J. (2002). Formation of modified DNA bases in cells exposed either to gamma radiation or to high-LET particles. Radiat. Res. *157*, 589–595.
22. Maremonti, E., Eide, D.M., Rossbach, L.M., Lind, O.C., Salbu, B., and Brede, D.A. (2020). In vivo assessment of reactive oxygen species production and oxidative stress effects induced by chronic exposure to gamma radiation in Caenorhabditis elegans. Free Radic. Biol. Med. *152*, 583–596.
23. Feinendegen, L.E., Pollycove, M., and Sondhaus, C.A. (2004). Responses to low doses of ionizing radiation in biological systems. Nonlinearity Biol. Toxicol. Med. *2*, 143–171.
24. Yadav, A., Monsieurs, P., Misztak, A., Waleron, K., Leys, N., Cuypers, A., and Janssen, P.J. (2019). Helical and linear morphotypes of Arthrospira sp. PCC 8005 display genomic differences and respond differently to 60Co gamma irradiation. Eur. J. Phycol. *55*, 129–146. https://doi.org/10.1080/09670262.2019.1675763.
25. Badri, H., Monsieurs, P., Coninx, I., Wattiez, R., and Leys, N. (2015). Molecular investigation of the radiation resistance of edible cyanobacterium

Arthrospira sp. PCC 8005. Microbiologyopen *4*, 187–207. https://doi.org/10.1002/mbo3.229.

26. Moussa, H., Ismaiel, M., Shabana, E., Gabr, M., and El-Shaer, E. (2015). The role of gamma irradiation on growth and some metabolic activities of Spirulina platensis. J. Nucl. Tech. Appl. Sci *3*, 99–107.
27. Planel, H., Soleilhavoup, J.P., Tixador, R., Richoilley, G., Conter, A., Croute, F., Caratero, C., and Gaubin, Y. (1987). Influence on cell proliferation of background radiation or exposure to very low, chronic gamma radiation. Health Phys. *52*, 571–578.
28. Yadav, A., Maertens, L., Meese, T., Van Nieuwerburgh, F., Mysara, M., Leys, N., Cuypers, A., and Janssen, P.J. (2021). Genetic Responses of Metabolically Active Limnospira indica Strain PCC 8005 Exposed to γ-Radiation during Its Lifecycle. Microorganisms *9*, 1626.
29. Upton, A.C. (2001). Radiation hormesis: data and interpretations. Crit. Rev. Toxicol. *31*, 681–695.
30. Mattson, M.P. (2008). Hormesis defined. Ageing Res. Rev. *7*, 1–7.
31. Liu, Y., Chen, X., Zhang, J., and Gao, B. (2015). Hormesis effects of amoxicillin on growth and cellular biosynthesis of Microcystis aeruginosa at different nitrogen levels. Microb. Ecol. *69*, 608–617.
32. Vallenet, D., Labarre, L., Rouy, Z., Barbe, V., Bocs, S., Cruveiller, S., Lajus, A., Pascal, G., Scarpelli, C., and Médigue, C. (2006). MaGe: a microbial genome annotation system supported by synteny results. Nucleic Acids Res. *34*, 53–65.
33. Robinson, C.K., Webb, K., Kaur, A., Jaruga, P., Dizdaroglu, M., Baliga, N.S., Place, A., and DiRuggiero, J. (2011). A major role for nonenzymatic antioxidant processes in the radioresistance of Halobacterium salinarum. J. Bacteriol. *193*, 1653–1662.
34. Daly, M.J., Gaidamakova, E.K., Matrosova, V.Y., Kiang, J.G., Fukumoto, R., Lee, D.-Y., Wehr, N.B., Viteri, G.A., Berlett, B.S., and Levine, R.L. (2010). Small-molecule antioxidant proteome-shields in Deinococcus radiodurans. PLoS One *5*, e12570.
35. Abomohra, A.E.-F., El-Shouny, W., Sharaf, M., and Abo-Eleneen, M. (2016). Effect of gamma radiation on growth and metabolic activities of Arthrospira platensis. Braz. Arch. Biol. Technol. *59*, e16150476.
36. Phukan, T., Rai, A.N., and Syiem, M.B. (2019). Unstandardized UV-C dose used for killing harmful cyanobacteria may instead initiate accelerated growth in the target organisms. Ecotoxicol. Environ. Saf. *181*, 274–283.
37. Kwon, J.-H., Bernát, G., Wagner, H., Rögner, M., and Rexroth, S. (2013). Reduced light-harvesting antenna: consequences on cyanobacterial metabolism and photosynthetic productivity. Algal Res. *2*, 188–195.
38. Van Hoeck, A., Horemans, N., Nauts, R., Van Hees, M., Vandenhove, H., and Blust, R. (2017). Lemna minor plants chronically exposed to ionising radiation: RNA-seq analysis indicates a dose rate dependent shift from acclimation to survival strategies. Plant Sci. *257*, 84–95.
39. Volkova, P.Y., Bondarenko, E.V., and Kazakova, E.A. (2022). Radiation Hormesis in Plants. Curr. Opin. Toxicol. *30*, 1–8.
40. Jantaro, S., and Kanwal, S. (2017). Low-molecular-weight nitrogenous compounds (GABA and polyamines) in blue–green algae. In Algal Green Chemistry (Elsevier), pp. 149–169.
41. Kotakis, C., Theodoropoulou, E., Tassis, K., Oustamanolakis, C., Ioannidis, N.E., and Kotzabasis, K. (2014). Putrescine, a fast-acting switch for tolerance against osmotic stress. J. Plant Physiol. *171*, 48–51.
42. Oh, T.J., and Kim, I.G. (1998). Polyamines protect against DNA strand breaks and aid cell survival against irradiation in Escherichia coli. Biotechnol. Tech. *12*, 755–758.
43. Lea-Smith, D.J., Bombelli, P., Vasudevan, R., and Howe, C.J. (2016). Photosynthetic, respiratory and extracellular electron transport pathways in cyanobacteria. Biochim. Biophys. Acta *1857*, 247–255.
44. Blahut, M., Sanchez, E., Fisher, C.E., and Outten, F.W. (2020). Fe-S cluster biogenesis by the bacterial Suf pathway. Biochim. Biophys. Acta. Mol. Cell Res. *1867*, 118829.
45. Gutekunst, K., Chen, X., Schreiber, K., Kaspar, U., Makam, S., and Appel, J. (2014). The bidirectional NiFe-hydrogenase in Synechocystis sp. PCC 6803 is reduced by flavodoxin and ferredoxin and is essential under mixotrophic, nitrate-limiting conditions. J. Biol. Chem. *289*, 1930–1937.
46. Yi, J., Xu, D., Zang, X., Yuan, D., Zhao, B., Tang, L., Tan, Y., and Zhang, X. (2014). Lyase activities of heterologous CpcS and CpcT for phycocyanin holo-β-subunit from Arthrospira platensis in Escherichia coli. J. Ocean Univ. China *13*, 497–502.
47. Liu, L.-N., Chen, X.-L., Zhang, Y.-Z., and Zhou, B.-C. (2005). Characterization, structure and function of linker polypeptides in phycobilisomes of cyanobacteria and red algae: an overview. Biochim. Biophys. Acta *1708*, 133–142.
48. Sanz-Luque, E., Bhaya, D., and Grossman, A.R. (2020). Polyphosphate: a multifunctional metabolite in cyanobacteria and algae. Front. Plant Sci. *11*, 938.
49. Jurgenson, C.T., Begley, T.P., and Ealick, S.E. (2009). The structural and biochemical foundations of thiamin biosynthesis. Annu. Rev. Biochem. *78*, 569–603.
50. Li, Z.-M., Hu, Z., Wang, X., Chen, S., Yu, W., Liu, J., and Li, Z. (2023). Biochemical and Structural Insights into a Thiamine Diphosphate-Dependent α-Ketoglutarate Decarboxylase from Cyanobacterium Microcystis aeruginosa NIES-843. Int. J. Mol. Sci. *24*, 12198.
51. Begley, T.P., Downs, D.M., Ealick, S.E., McLafferty, F.W., Van Loon, A.P., Taylor, S., Campobasso, N., Chiu, H.-J., Kinsland, C., Reddick, J.J., and Xi, J. (1999). Thiamin biosynthesis in prokaryotes. Arch. Microbiol. *171*, 293–300.
52. Tandon, P., Jin, Q., and Huang, L. (2017). A promising approach to enhance microalgae productivity by exogenous supply of vitamins. Microb. Cell Fact. *16*, 219.
53. Helliwell, K.E., Lawrence, A.D., Holzer, A., Kudahl, U.J., Sasso, S., Kräutler, B., Scanlan, D.J., Warren, M.J., and Smith, A.G. (2016). Cyanobacteria and eukaryotic algae use different chemical variants of vitamin B12. Curr. Biol. *26*, 999–1008.
54. Wagner, C. (2001). Biochemical role of folate in cellular metabolism. Clin. Res. Regul. Aff. *18*, 161–180.
55. Mills, L.A., McCormick, A.J., and Lea-Smith, D.J. (2020). Current knowledge and recent advances in understanding metabolism of the model cyanobacterium Synechocystis sp. PCC 6803. Biosci. Rep. *40*, BSR20193325.
56. Waldrop, G.L., Holden, H.M., and Maurice, M.S. (2012). The enzymes of biotin dependent CO2 metabolism: what structures reveal about their reaction mechanisms. Protein Sci. *21*, 1597–1619.
57. Estévez, J.M., Cantero, A., Reindl, A., Reichler, S., and León, P. (2001). 1-Deoxy-D-xylulose-5-phosphate synthase, a limiting enzyme for plastidic isoprenoid biosynthesis in plants. J. Biol. Chem. *276*, 22901–22909.
58. Nowicka, B., and Kruk, J. (2010). Occurrence, biosynthesis and function of isoprenoid quinones. Biochim. Biophys. Acta *1797*, 1587–1605.
59. Schuergers, N., Mullineaux, C.W., and Wilde, A. (2017). Cyanobacteria in motion. Curr. Opin. Plant Biol. *37*, 109–115.
60. Miklaszewska, M., Waleron, M., Morin, N., Calusinska, M., Wilmotte, A., Tandeau De Marsac, N., Rippka, R., and Waleron, K. (2012). Elucidation of the gas vesicle gene clusters in cyanobacteria of the genus Arthrospira (Oscillatoriales, Cyanophyta) and correlation with ITS phylogeny. Eur. J. Phycol. *47*, 233–244.
61. Tyanova, S., Temu, T., and Cox, J. (2016). The MaxQuant computational platform for mass spectrometry-based shotgun proteomics. Nat. Protoc. *11*, 2301–2319.
62. Cox, J., and Mann, M. (2008). MaxQuant enables high peptide identification rates, individualized ppb-range mass accuracies and proteome-wide protein quantification. Nat. Biotechnol. *26*, 1367–1372.
63. Kammers, K., Cole, R.N., Tiengwe, C., and Ruczinski, I. (2015). Detecting significant changes in protein abundance. EuPA Open Proteom. *7*, 11–19.

64. Cogne, G., Lehmann, B., Dussap, C.G., and Gros, J.B. (2003). Uptake of macrominerals and trace elements by the cyanobacterium Spirulina platensis (Arthrospira platensis PCC 8005) under photoautotrophic conditions: culture medium optimization. Biotechnol. Bioeng. *81*, 588–593. https://doi.org/10.1002/bit.10504.

65. Miller, A.G., and Colman, B. (1980). Evidence for HCO3− transport by the blue-green alga (cyanobacterium) Coccochloris peniocystis. Plant Physiol. *65*, 397–402.

66. Schreiber, U., Endo, T., Mi, H., and Asada, K. (1995). Quenching analysis of chlorophyll fluorescence by the saturation pulse method: particular aspects relating to the study of eukaryotic algae and cyanobacteria. Plant Cell Physiol. *36*, 873–882.

67. Aguirre-von-Wobeser, E., Figueroa, F.L., and Cabello-Pasini, A. (2000). Effect of UV radiation on photoinhibition of marine macrophytes in culture systems. J. Appl. Phycol. *12*, 159–168.

68. Schuurmans, R.M., van Alphen, P., Schuurmans, J.M., Matthijs, H.C.P., and Hellingwerf, K.J. (2015). Comparison of the photosynthetic yield of cyanobacteria and green algae: different methods give different answers. PLoS One *10*, e0139061.

69. Gao, K., Yu, H., and Brown, M.T. (2007). Solar PAR and UV radiation affects the physiology and morphology of the cyanobacterium Anabaena sp. PCC 7120. J. Photochem. Photobiol., B *89*, 117–124.

70. Masojídek, J., Vonshak, A., and Torzillo, G. (2010). Chlorophyll fluorescence applications in microalgal mass cultures. In Chlorophyll a fluorescence in aquatic sciences: methods and applications (Springer), pp. 277–292.

71. Allahverdiyeva, Y., Mustila, H., Ermakova, M., Bersanini, L., Richaud, P., Ajlani, G., Battchikova, N., Cournac, L., and Aro, E.-M. (2013). Flavodiiron proteins Flv1 and Flv3 enable cyanobacterial growth and photosynthesis under fluctuating light. Proc. Natl. Acad. Sci. USA *110*, 4111–4116.

72. Bennett, A., and Bogorad, L. (1973). Complementary chromatic adaptation in a filamentous blue-green alga. J. Cell Biol. *58*, 419–435.

73. Phélippé, M., Gonçalves, O., Thouand, G., Cogne, G., and Laroche, C. (2019). Characterization of the polysaccharides chemical diversity of the cyanobacteria Arthrospira platensis. Algal Res. *38*, 101426.

74. Deutsch, E.W., Bandeira, N., Perez-Riverol, Y., Sharma, V., Carver, J.J., Mendoza, L., Kundu, D.J., Wang, S., Bandla, C., Kamatchinathan, S., et al. (2023). The ProteomeXchange consortium at 10 years: 2023 update. Nucleic Acids Res. *51*, D1539–D1548.

75. Perez-Riverol, Y., Bai, J., Bandla, C., García-Seisdedos, D., Hewapathirana, S., Kamatchinathan, S., Kundu, D.J., Prakash, A., Frericks-Zipper, A., Eisenacher, M., et al. (2022). The PRIDE database resources in 2022: a hub for mass spectrometry-based proteomics evidences. Nucleic Acids Res. *50*, D543–D552.

STAR★METHODS

KEY RESOURCES TABLE

REAGENT or RESOURCE	SOURCE	IDENTIFIER
Bacterial and virus strains		
Limnospira indica PCC8005 P3	SCK CEN	-
Deposited data		
Proteomics data sets	ProteomeXchange	PXD051709 (https://doi.org/10.6019/PXD051709)
Software and algorithms		
MaxQuant software (version 2.0.1.0)	Max-Plank Institute of Biochemistry, Department of Proteomics and Signal Transduction, Munich, Germany	https://www.maxquant.org/
Bruker Compass Hystar software (version 6.2)	Bruker Daltonics, Bremen, Germany	https://www.bruker.com/en/products-and-solutions/mass-spectrometry/lc-ms/compass-hystar.html
Bruker otofControl software (Version 6.3)	Bruker Daltonics, Bremen, Germany	-
Andromeda search engine	Tyanova et al.[61] and Cox and Mann[62]	https://doi.org/10.1021/pr101065j
in-house python script	SCK CEN	-
LIMMA R package	Kammers et al.[63]	-

EXPERIMENTAL MODEL AND STUDY PARTICIPANT DETAILS

Limnospira indica PCC8005 strain P3 was grown in Zarrouk medium as modified by Cogne, Lehmann, Dussap and Gros.[64] Thus, dissolved bicarbonate was used as the sole carbon source and nitrate as the sole nitrogen source. The P3 strain used in this study is adapted to low light conditions (25-45 μmol photons m^{-2} s^{-1}), constant illumination (no day/night cycle), constant shaking at 120 rpm and warm temperatures (30°C) by long-term batch growth in Zarrouk medium under these conditions in the laboratory. More information on the characteristics and microscopy pictures of the strain can be found in Fahrion, Dussap and Leys.[3]

In total, eight 250 mL Erlenmeyer flasks were filled with 7.5 mL of culture and 142.5 mL of Zarrouk at the beginning of each batch in experiment 1 (5 %v/v inoculation), and with 37.5 mL of culture and 112.5 mL of Zarrouk in the beginning of the batches of experiment 2 (25 %v/v inoculation). Four flasks were used as non-irradiated control, four were exposed to the irradiated environment. In both experiments, the culture of the previous batch was used for the following inoculation, to test the cumulative irradiation effects over multiple consecutive cell generations over the course of eight weeks. In experiment 1 (exp. 1), one batch lasted two weeks (= 4 batches in total) and in experiment 2 (exp. 2), one batch lasted one week (= 8 batches in total). Four biological replicate cultures were grown in parallel.

The cultures were put in 2 LED towers (in-house built at SCK CEN, 1 for non-irradiated control cultures, 1for irradiated cultures, using SMD-LED warm white 1300 mcd, type NESL064AT, Nichia Corporation, Tokushima, Japan) and covered with a dark plastic sheet to secure that the LEDs are the only light source. The set-up is illustrated in Figure 8. This set-up was already used in our previous studies.[28] The LED towers provided the cultures with full PAR (400-700 nm) in a 24/7 regime; thus, no day/night cycle was performed. The LED towers with the cultures were put on orbital shakers (Edmund Bühler GmbH) at 120 rpm to prevent cell sedimentation and increase light exposure. The irradiation set-up was positioned on a small trolley in the same room as the cobalt^{60} source (Laboratory for Nuclear Calibrations at SCK CEN). The control set-up was positioned in a room in the same building to secure similar temperature, pressure, and humidity levels. The ambient temperature in the irradiation and control rooms was controlled regularly and found to be stable at 25 ± 2°C. Due to the natural decay of the Co^{60} source between experiment 1 and 2, the dose rate in experiment 2 was slightly lower than in experiment 1. The irradiation dose was measured with dosimeters for 48 and 46 hours respectively, during both experiments (supplementary data Table S1). The dosimetry measurements in this study revealed actual dose rates of 85.2 μSv h^{-1} (=70.4 μGy h^{-1}, γ-rays, experiment 1) and 63.5 μSv h^{-1} (=52.5 μGy h^{-1}, γ-rays, experiment 2) (supplementary data Table S1). Due to logistic constraints in the irradiation facility used, only the first 2 months (8 weeks) of the full length of ca. 10 months (ca. 300 days) of a transit to Mars could be tested. The cultures were irradiated for a total of 8 weeks, resulting in cumulative doses of 94.6 mGy and 70.6 mGy. Entrance of experimenters to the irradiation room was limited to 1-2x per week, and as such also sampling limiting the data points to 1-2 per week in the analyses performed.

METHOD DETAILS

Optical density, dry weight and pH measurements

Three methods were used to assess the biomass production. Firstly, the optical density (absorbance at 770nm (OD_{770nm})) of the cultures was measured up to 4 times a week using a NANOCOLOR® UV/VIS II spectrophotometer (MACHEREY-NAGEL) and semi-micro cuvettes (Greiner BIO-ONE). At the end of a batch (dotted lines in Figure 1), the starting OD of a new batch was calculated using the final OD values of the previous batch and the inoculation percentage (5% in experiment 1 and 25% in experiment 2). Whenever possible, the OD measurements were performed 3 times on each of the 4 biological replicate to account for the measurement error of the spectrophotometer.

Secondly, the biomass dry weight of the cultures was assessed by filtering 2 mL of culture on pre-weighed membrane disc filters (water wettable PTFE, Pall Laboratory, pore size 45μm, ⌀ 25mm). On each time point, 3 filters were used per culture (3 technical replicates), resulting in a total of 12 filters for the 4 parallel replicate cultures per condition. The dry weight could not be assessed at time point zero of a batch, because previous work in our laboratory showed that the dry weight assessment becomes less accurate at lower cell concentrations.

The biomass production rate r_X [g L^{-1} d^{-1}] was obtained via linear regression of the dry weight measurements in Excel 2016 data analysis toolpak. The linear regressions were performed for each batch and the r_X values are displayed as mean ± 95% confidence interval (CI).

Thirdly, the pH was measured with a KCl pH electrode (InLab®, Mettler Toledo). Because of the bicarbonate uptake of the cultures, the pH increases when biomass concentration increases. This information is used as an additional assessment of the growth (supplementary material Figure S1).[2,3,65]

Flow cytometry

Flow cytometry measurements were performed using an ACCURI C6 flow cytometer (BD Biosciences), which is equipped with a blue (488nm) and a red (640nm) laser. Aliquots of 100 μl of a 1:5 diluted *Limnospira* culture (in Zarrouk) were run in fast mode using the following thresholds: 10,000 in the forward scatter (FSC-H) and 800 in the fluorescent detector 4 (FL4-H), using the modified Zarrouk medium as blank background. In this study, only the percentage of the so-called P1 cells (highly pigmented and long trichomes) regarding the total cell count was assessed (called %P1 from now on). The abundance of cells in this area was proven to be essential to start photosynthetic growth of *Limnospira indica* PCC8005 P3 after frozen storage by previous work of our laboratory (unpublished data) and the percentage of P1 cells was shown to influence the outcome of storage of *Limnospira indica* in liquid zarrouk medium under dark and cold (4°C) conditions (F.M., unpublished data).

Phothosynthesis quantum yield measurement

The chlorophyl fluorescence and the photosynthetic quantum yield (QY) of PSII was determined by pulse amplitude modulated (PAM) fluorimetry[66–68] using an AquaPen-C AP 110-C (Photon System Instruments PSI). The measurement was done according to the fixed values in the AquaPen-C manual, with a flash pulse of 30% (900 μmol photons m^{-2} s^{-1}, red LED with peak at 630 nm, 30 μs) as measuring light to determine minimal fluorescence F_t and a super pulse of 70% (2,100 μmol photons m^{-2} s^{-1}, red LED with peak at 630 nm, 1 s) as measuring light to determine maximal fluorescence F_m. The AquaPen-C device calculates the $\Delta F/F_m$ ratio and gives the QY value as output. The QY ($\Delta F/F_m$) is defined as:

$$QY = \frac{F_m - F_t}{F_m} \quad \text{(Equation 1)}$$

Where F_m is the maximal fluorescence and F_t is the minimum fluorescence, both for dark adapted cells (20 min dark). Previous studies showed that the QY values for cyanobacteria in active photosynthetic growth usually lie between 0.3 and 0.6.[68–71] Previous work from our laboratory found that the *L. indica* PCC8005 strain P3 usually yields QY values between 0.3 and 0.5 (dark adapted).[3] QY represents the efficiency of photochemistry in PSII and can be used for qualitative comparison of photosynthetic efficiency of individual cultures.

Pigment analysis

Samples for pigment analysis were taken every week. The concentrations of phycocyanin (phy), allophycocyanin (apc) and chlorophyll a (chl) were measured as weight fraction versus the dry weight (mg/mg DW, % w/w) using a spectrophotometric method. The extraction protocol is a slightly modified version of the protocol in Badri, Monsieurs, Coninx, Wattiez and Leys[25] and is based on the calculations of Bennett and Bogorad.[72] Briefly, the frozen cell pellets of 2 ml of culture were suspended in 1 mL of 0.05 M Na_2HPO_4 at pH 7. Thereafter, 5 cycles of freezing in liquid N_2 and thawing at 37°C in a water bath were performed to crack the cells. Next, 100 μL lysozyme (100 mg/ml) were added and the tubes were incubated for 30 min at 37°C. The tubes were centrifuged at 13,000 g for 10 min and the supernatant was measured with a NANOCOLOR® UV/VIS II spectrophotometer for absorbance at 615 nm and 652 nm, to determine the concentrations of phycobilliprotein antenna pigments (phy, apc) in the extract. The extraction of chlorophyll was performed on the remaining pellet of the phycobilliprotein extraction. Firstly, the pellets were washed three times using 0.05 M Na_2HPO_4 at pH 7. Then, 1 mL of 100% methanol was used to extract the organic soluble pigment chlorophyll. Three cycles of ultra-sonication

(30 kHz, 10 s, amplitude 30%, 1 pulse per second, Hielscher Ultrasound Technology, UP50H) were performed to fully extract and dissolve the chlorophyll pigments. Centrifugation at 4°C for 10 min at 13,000 g was performed to remove cell debris, and the supernatant was measured at 665 nm using a NANOCOLOR® UV/VIS II spectrophotometer (MACHEREY-NAGEL) and semi-micro cuvettes (Greiner BIO-ONE) to determine the chlorophyll concentration in the extract. The spectrophotometric measurements were performed 3 times on each of the 4 biological replicate to account for the measurement error of the spectrophotometer. Additionally, the concentration of carotenoids was assessed according to the protocol of Abomohra, El-Shouny, Sharaf and Abo-Eleneen.[35] The carotenoids were extracted by adding 1 ml of 100% methanol to the frozen samples (stored at -80°C, pellets from 2 mL of culture) and subsequently heating them at 55°C for 15 min using a heating block. The absorbance of the resulting supernatant was measured at 452, 665, and 650 nm using semi-micro cuvettes (Greiner BIO-ONE) and a NANOCOLOR® UV/VIS II spectrophotometer (MACHEREY-NAGEL). To calculate the total carotenoid concentration (CAR), the following equation was used:

$$CAR\ (\mu g\ ml^{-1}) = 4.2 \times A_{452nm} - [0.0246 \times (10.3 \times A_{665nm} - 0.918 \times A_{650nm})] \quad \text{(Equation 2)}$$

where A_{452nm}, A_{665nm}, and A_{650nm} are the absorbance values at 452, 665, and 650 nm, respectively. Similar to the other pigments, the carotenoid content was normalized by the dry weight (μg/mg DW).

Glycogen analysis

The glycogen content was investigated spectrophotometrically using a modified protocol of Phélippé et al.[73] In short, the thawed pellet of 2ml of culture was suspended in 1mL 100%methanol and incubated at 45°C for 45min in a heating block (550 rpm). The suspension was then centrifuged at room temperature for 10 min at 12,000 g and the supernatant was discarded. The pellet containing the glycogen was resuspended in 200 μl of 30% KOH solution. Now the suspension was incubated at 90°C in a heating block for 30 min (550 rpm). The suspension was cooled down to room temperature and 600 μl pre-chilled (4°C) 100% ethanol was added to precipitate the glycogen. The samples were stored at −20°C for 1 h. Afterwards, the samples were centrifuged at room temperature for 5 min at 12,000 g and the supernatant was discarded. The pellet was washed 2 times with 600 μl pre-chilled (4°C) 100% ethanol. Then, the pellet was dried at 60°C in a heating block for 10min to evaporate the ethanol (open lid). The dried pellet was resuspended in 100 μl 100mM sodium acetate buffer + 5mM calcium chloride at pH 4.5. 20 μl of amyloglucosidase enzyme solution (3300 U/ml) was added (Total Starch Assay, Megazyme) and the suspension was incubated at 60°C in a heating block (550 rpm) for 15 min (enzymatic hydrolysis of glycogen into glucose). Then, the samples were split into two aliquots of 50 μL and 800 μL hexokinase (GlucoseAssayReagent, G3293, Sigma-Aldrich) was added to one of the aliquots. This suspension was incubated at room temperature for 15 min. The sample blank consisted of the other 50 μL aliquot and 800 μL ddH2O and the reagent blank was made using 50 μL ddH_2O and 800 μL hexokinase solution. A calibration curve was created using pure glycogen from algae (Megazyme) in MilliQ as a standard. The absorbance (A340) of the blanks and samples was measured with the NANOCOLOR® UV/VIS II spectrophotometer (MACHEREY-NAGEL) at λ = 340 nm using semi-micro cuvettes (greiner BIO-ONE). The glycogen content was determined using the standard curve. Based on literature, glycogen content varies extremely depending on the culturing conditions. The glycogen content was normalised by the dry weight (mg/mg DW).

Proteome analysis

Protein extraction and quantification

The proteins were extracted by dissolving a 15 ml culture cell pellet in twice its volume of 2% SDS in 50mM Ammonium BiCarbonates (ABC) solution. The mixture was vortexed for 3 times for 10 seconds until the pellet was fully dissolved. The solution was transferred to a 1.5 ml Eppendorf tube and incubated in a heating block for 5 minutes at 95°C. Afterwards, the tube was cooled on ice for 5 minutes, followed by a brief centrifugation (∼5s). Then, the sample was lysed by ultrasonication (4 times for 10 s, amplitude 40%, in between 1 min on ice) (Imlab, Boutersem, Belgium). After sonication, the sample was centrifuged for 20 minutes at 14,000 rpm and 4°C. Lastly, the supernatant was transferred to a new Eppendorf tube and the protein quantification was carried out using the BCA assay (Merck Life Science BV, Hoeilaart, Belgium) following the manufacturer's instructions.

Mass spectrometry analysis

Extracted proteins were further processed for LC-MS/MS analysis using the suspension trapping method (S-trap) (Bioconnect, Huissen, The Netherlands) following the manufacturer's instructions. Next, LC-MS/MS analysis was performed using a nanoElute UHPLC (Bruker Daltonics, Bremen, Germany), via a CaptiveSpray nanoflow electrospray source (Bruker Daltonics, Bremen, Germany), connected to a QTOF-MS instrument (Impact II, Bruker Daltonics, Germany). Samples were run in a random order to exclude a potential batch effect. In total, 2 μg of tryptic digest (in 0.1% formic acid in water) was injected onto a trapping column setup (300 μm x 5 mm, C18 PepMap 300, 5 μm, 100 Å; Bruker Daltonics, Bremen, Germany). Subsequently, peptides were separated using a C18 Reprosil AQ, 1.9 μm, 120 Å, 0.075 x 150 mm column operated at 40°C (Bruker Daltonics, Bremen, Germany) at a flow rate of 0.2 μL/min. Gradient conditions were: 2–35% 0.1% formic acid in acetonitrile for 100 min; 35–95% 0.1% formic acid in acetonitrile for 10 min; 95% 0.1% formic acid in acetonitrile held for 10 min. Drying gas flow and temperature of the CaptiveSpray were set to 4 L/min and 180°C, respectively, and nebulizer gas pressure was set to 0.4 bar. MS acquisition rate was set to 2 Hz and data have been acquired over a 150–2200 m/z mass range. In all the full-scan measurements, a lock-mass (m/z 1221.9906, Hexakis (1H, 1H, 4H-hexafluorobutyloxy) phosphazine) (Bruker Daltonics, Bremen, Germany) was used as internal calibrator.

Instant Expertise method (Compass otofSeries 4.1, Bruker Daltonics, Bremen, Germany) was used to select as many as possible of the most intense ions per cycle of 3 s MS/MS accumulation depended on the MS1 level. Threshold (per 1,000 summation) absolute was 2,500 cts (spectral rate of 2 Hz). Peptide fragmentation was performed with nitrogen gas on the most abundant and at least doubly charged to five charged ions detected in the initial MS scan. Active exclusion was performed after 1 spectrum for 0.50 min unless the intensity of the precursor ions was more than 3 times higher than in the previous scan. The mass spectrometry proteomic data were submitted to the ProteomeXchange Consortium[74] via the PRIDE[75] partner repository with the dataset identifiers PXD051709 (https://doi.org/10.6019/PXD051709).

Mass spectrometry raw data processing

All raw mass spectrometry spectra files were processed using MaxQuant software version 2.0.1.0 (Max-Plank Institute of Biochemistry, Department of Proteomics and Signal Transduction, Munich, Germany) and the proteins were identified with the built-in Andromeda search engine.[61,62] For both irradiation experiments, 16 raw files, with 4 replicates of each of the 4 conditions (i.e. non-irradiated control 4 weeks, non-irradiated control 8 weeks, irradiated 4 weeks and irradiated 8 weeks) were processed in parallel, resulting in a total of 32 raw files. The database searches were performed against a database containing all *Limnospira indica* PCC 8005 protein sequences, downloaded from the MaGe platform on 2023-03-23.[32] Default MaxQuant parameter settings were used: cysteine carbamidomethylation as fixed modification, and methionine oxidation and Protein N-terminal acetylation, as variable modification; False-discovery rate (FDR) cutoffs set to 1% on peptide, protein, and site decoy level; trypsin as a digestion enzyme; 7 amino acids as minimum peptide length.

Normalization and filtering of proteomic data

The resulting protein data from MaxQuant analysis with minimum 2 unique peptides were retained and were processed to remove reverse hits and contaminants from the data. Then intensities were transformed to log2 for further analysis. To remove the technical variation among replicates, median normalization on log2-transformed intensities was performed using an in-house python script.[61,63] Missing values in the data were replaced by value from a normal distribution with settings width =0.3 and downshift =1.8. Protein differential expression was calculated using LIMMA R package,[63] based on the empirical Bayes moderated test-statistics. The expression was considered significant at a p-value <0.05 and a fold-change greater than 1.5 and smaller than 0.66 (log2FC > 0.5849 and < -0.5849).

QUANTIFICATIONS AND STATISTICAL ANALYSIS

Statistical significance was assessed by Mann-Whitney-U tests (nonparametric) using Graphpad Prism 9. The symbol * indicates time points where the irradiated cultures had a significant higher value compared to the non-irradiated cultures in the tested parameter; the symbol # indicates time points where the irradiated cultures had a significant lower value compared to the non-irradiated cultures. The threshold for significance was */#: $p < 0.05$. For the OD and dry weight measurements, the statistical analysis was performed using all 12 replicates (4 biological and 3 technical each), as well as by averaging the technical replicates and statistical analysis of only the 4 biological replicates (n=4). Similar results were found, thus, the statistical results including the separate technical replicates are shown (n=12). The biomass production rates were assessed differently because they were obtained via linear regression using the excel data analysis toolpak. The biomass production rate values are shown as mean ± 95%CI. Statistical significance was assessed based on overlapping 95%CI.